Title

Design, Characterization, and Use of a Novel Amyloid β-Protein Control for Assembly, Neurotoxicity, and Gene Expression Studies

Journal

Biochemistry, 55(36)

ISSN

0006-2960

Authors

Yamin, Ghiam
Coppola, Giovanni
Teplow, David B

Publication Date

2016-09-13

DOI

10.1021/acs.biochem.6b00579

Peer reviewed

BIOCHEMISTRY
including biophysical chemistry & molecular biology

Article

Design, characterization, and use of a novel amyloid #-protein control for aggregation and neurotoxicity assays

Ghiam Yamin, Giovanni Coppola, and David B Teplow

Biochemistry, **Just Accepted Manuscript** • DOI: 10.1021/acs.biochem.6b00579 • Publication Date (Web): 09 Aug 2016

ACS Publications

Biochemistry is published by the American Chemical Society. 1155 Sixteenth Street N.W., Washington, DC 20036

Design, characterization, and use of a novel amyloid β-protein control for assembly, neurotoxicity, and gene expression studies

Ghiam Yamin[a, b], Giovanni Coppola[b, c], and David B. Teplow[b*]

[a]Department of Radiology, University of California San Diego School of Medicine, La Jolla, CA; [b]Department of Neurology, David Geffen School of Medicine at UCLA, Los Angeles, CA; [c]Department of Psychiatry and Semel Institute for Neuroscience and Human Behavior, David Geffen School of Medicine at UCLA, Los Angeles, CA

[*]Address correspondence to: Dr. David B. Teplow, Department of Neurology, David Geffen School of Medicine at UCLA, 635 Charles E. Young Drive South, Room 445, Los Angeles, CA 90095, USA, Phone: 310-206-2030, Fax: 310-206-1700, Email: dteplow@mednet.ucla.edu.

Running Title: Aβ aggregation and neurotoxicity control

Abbreviations and Textual Footnotes

Aβ	Amyloid β-protein
AD	Alzheimer's disease
APS	Ammonium persulfate
CD	Circular dichroism
ds cDNA	Double stranded cDNA
TO	Topological overlap
DDI	Double-distilled de-ionized
DIV	Days *in vitro*
DTT	Dithiothreitol
FBS	Fetal bovine serum
Fmoc	9-fluorenylmethoxycarbonyl
FU	Arbitrary fluorescence units
HC	Hippocampal
HS	Horse serum
LMW	Low molecular weight
MTT	3-[4,5-dimethylthiazol-2-yl]-2,5-diphenyltetrazolium bromide
MWCO	Molecular weight cut-off
NGF	Nerve growth factor
NFT	Neurofibrillary tangles
NOS	Nitric oxide synthase
PC12	Rat pheochromocytoma
pI	Isoelectric point

PICUP	**Photo-induced cross-linking of unmodified proteins**
P/S	**Penicillin/streptomycin**
RIN	**Sample RNA integrity**
Ru(Bpy)3	**Tris(2,2-bipyridyl)dichlororuthenium(II) hexahydrate**
SAR	**Structure-activity relationship**
sAβ40	**YHAGVDKEVVFDEGGAEHGLAQKIVRGFGVSDVSMIHNLF**
sAβ42	**YHAGVDKEVVFDEGAGAEHGLAQKIVRGFGVSDVSMIHINLF**
SDS-PAGE	**Sodium dodecyl-polyacrylamide gel electrophoresis**
ThT	**Thioflavin T**
TO	**Topological overlap**
v/v	**Volume to volume**
WGCNA	**Weighted gene co-expression network analysis**

Abstract

A key pathogenic agent in Alzheimer's disease (AD) is the amyloid β-protein (Aβ), which self-assembles into a variety of neurotoxic structures. Establishing structure-activity relationships for these assemblies, which is critical for proper therapeutic target identification and design, requires aggregation and neurotoxicity experiments that are properly controlled with respect to the Aβ peptide itself. "Reverse" Aβ or non-Aβ peptides suffer from the fact that their biophysical properties are too similar or dissimilar, respectively, to native Aβ for them to be appropriate controls. For this reason, we used simple protein design principles to create scrambled Aβ peptides predicted to behave distinctly from native Aβ. We showed that our prediction was true by monitoring secondary structure dynamics with Thioflavin T fluorescence and circular dichroism spectroscopy, determining oligomer size distributions, and assaying neurotoxic activity. We then demonstrated the utility of the scrambled Aβ peptides by using them to control experiments examining the effects of Aβ monomers, dimers, higher-order oligomers, and fibrils on gene expression in primary rat hippocampal neurons. Significant changes in gene expression were observed for all peptide assemblies, but fibrils induced the largest changes. Weighted gene co-expression network analysis revealed two predominant gene modules related to Aβ treatment. Many genes within these modules were associated with inflammatory signaling pathways.

Alzheimer's disease (AD) is the most common late-life neurodegenerative disorder [1], affecting >5 million people in the United States and >27 million people worldwide [2]. AD is predominantly a disease of the aged, as >95% of patients are ≥65 years of age. Patients generally present initially with memory deficits, which then are followed by an inexorable decline in executive function and other mental abilities. AD is characterized histopathologically by intraneuronal neurofibrillary tangles (NFTs) formed by the microtubule-associating protein tau and by extraneuronal amyloid plaques formed by the amyloid β-protein (Aβ) [1]. Two alloforms of Aβ predominate in humans, Aβ40, which contains 40 amino acids, and Aβ42, which contains 42 amino acids [3]. Cerebrovascular amyloid deposits have an abundance of Aβ40, whereas the Aβ component of parenchymal plaques contains primarily Aβ42 [4, 5]. Plaque formation is associated with development and progression of AD [6]. For this reason, myriad studies have sought to elucidate the pathway(s) of Aβ fibril formation so that therapeutic agents could be targeted to those steps critical in the process. In doing so, an array of smaller Aβ assemblies, including low-order oligomers, annuli, globulomers, and protofibrils has been revealed [7]. This has led quite naturally to the determination of structure-activity relationships (SAR), which has shown that Aβ oligomers appear to be key neurotoxins [7-9].

We hypothesize that a neuron's ability to protect itself from the effects of Aβ oligomers, and other Aβ assemblies, is determined by age-related changes in the transcription of specific genes. As a first step to testing this hypothesis, we sought to use gene microarrays to determine gene expression changes induced in embryonic primary hippocampal (Hc) neuron cultures by monomers, oligomers, protofibrils, or fibrils formed by Aβ40 or Aβ42. However, a necessary prerequisite for performing these experiments were appropriate Aβ40 and Aβ42 control peptides, which would allow differentiation of gene expression changes due to the effects Aβ assemblies from those changes due to generic peptide:neuron interactions. We report here the design of such peptides, comparative

analysis of their structures and assembly behaviors, and their initial use in gene microarray experiments.

Experimental Procedures

Chemicals and Reagents

Unless specified otherwise, all chemicals and sera were obtained from Sigma-Aldrich (St. Louis, MO) and were of the highest purity available. Tris(2,2′-bipyridyl)dichlororuthenium(II) hexahydrate ($Ru(Bpy)_3$), ammonium persulfate (APS), Novex® 10-20% Tricine SDS gels, Neurobasal A media, B27 growth factor, glutamine, Penicillin/Streptomycin Solution were purchased from Invitrogen (Carlsbad, CA). Trypsin-EDTA (2.5% w/v) was obtained from ATCC (Manassas, VA). Scalpels were purchased from Sigma Aldrich. All solutions were prepared in double-distilled de-ionized (DDI) water produced using a Milli-Q system (Millipore Corp., Bedford, MA).

Peptide Design

Word scrambler software (http://www.lerfjhax.com/scrambler) was used to randomly permute the Aβ amino acid sequence. We then used Kyte-Doolittle analysis [10] with a window size of 9 (http://web.expasy.org/protscale/) to determine the hydropathy profiles of these permuted sequences (Fig. 1). The scrambled Aβ peptides below are identical to their cognate native Aβ peptides in length, pI, and amino acid composition, but they are not amphipathic.

Scrambled Aβ40 (sAβ40): YHAGVDKEVVFDEGGAEHGLAQKIVRGFGVSDVSMIHNLF

Scrambled Aβ42 (sAβ42): YHAGVDKEVVFDEGAGAEHGLAQKIVRGFGVSDVSMIHINLF

Peptide Synthesis

All peptides were synthesized using 9-fluorenylmethoxycarbonyl (Fmoc) chemistry, purified by

reverse phase-high performance liquid chromatography, and characterized by mass spectrometry and amino acid analysis, as described previously [7]. Quantitative amino acid analysis and mass spectrometry yielded the expected compositions and molecular weights, respectively, for each peptide. Purified peptides were stored as lyophilizates at -20°C.

Preparation of Low Molecular Weight (LMW), Oligomeric, and Fibrillar Aβ

Low molecular weight (LMW) Aβ comprises a mixture of Aβ monomers and dimers that exist in equilibrium [11]). Chemically stabilized oligomers were prepared using the method of Photo-Induced Cross-linking of Unmodified Proteins (PICUP), as described [10, 11]. Briefly, Aβ lyophilizates were dissolved in 10 mM sodium phosphate, pH 7.5, at a concentration of 80 μM and cross-linked by mixing 36 μL of protein solution with 2 μL of 2 mM Ru(Bpy)3 and 2 μL of 40 mM APS. The final Aβ:Ru(Bpy)3:APS molar ratios were 0.72:1:20. The mixture was irradiated for 1 s with visible light from a 150 W fiber optic illuminator (model 170-D, Dolan-Jenner, Lawrence, MA, USA), after which the reaction was quenched with 2 μL of 1 M dithiothreitol (DTT). Cross-linking reagents were removed using a Zeba Spin Desalting Column, 7K MWCO (Thermo Fisher Scientific, Rockford, IL). SDS-PAGE and silver staining were used to determine the frequency distribution of Aβ oligomers. This was accomplished by diluting the PICUP-treated Aβ to a concentration of 40 μM. Twenty-one μL of each cross-linked sample mixed with 21 μL of 2× SDS sample buffer was boiled for 10 min. Thereafter, 8 μL of each boiled cross-linked sample was electrophoresed on a 10-20% gradient Tricine gel (Invitrogen, Carlsbad, CA) and visualized by silver staining (SilverXpress, Invitrogen). Cross-linked Aβ40 and Aβ42 have distinct oligomer distributions that differ from distributions obtained in the absence of cross-linking (see Results and [12]). These distributions also differ from those obtained by preparation of oligomers using methods that do not stabilize the non-covalent interactions mediating the oligomerization process [13-17]. Non-cross-linked samples were used as

controls in each experiment. Fibrils were prepared by gently agitating a 1 mg/mL solution of LMW Aβ in 10 mM sodium phosphate, pH 7.5, at 37°C for 1 week. Non-fibrillar assemblies were removed by filtration using a 50 kDa molecular weight cut-off (MWCO) centricon filter. We note that the results obtained using the four different classes of Aβ assemblies prepared here are valid for determination of SAR, as the structures of each class are known. However, the relationships determined here may, or may not, match those determined in other systems because the Aβ preparations differ.

Circular Dichroism

Aβ samples were prepared in 10 mM sodium phosphate, pH 7.5, at a concentration of 50 μM and incubated at 37°C in 1-mm path length quartz cuvettes (Hellma, Forest Hills, NY). CD spectra were acquired using a J-810 spectropolarimeter (JASCO, Tokyo, Japan). Following temperature equilibration, spectra were recorded at 22°C from 195–260 nm at 0.2 nm resolution with a scan rate of 100 nm/min. Spectra were acquired immediately after sample preparation and then periodically for two weeks thereafter. Eight scans were acquired and averaged for each sample at each time point. Buffer spectra were subtracted from appropriate experimental spectra prior to data analysis.

Thioflavin T (ThT) Assay

ThT fluorescence was used to monitor β-sheet formation. Peptides were incubated at a final concentration of 50 μM in 10 mM sodium phosphate, pH 7.5. All assay solutions contained 20 μM ThT. One-hundred μL of each sample were placed into each of three wells (triplicates) of a white plastic, clear-bottomed, 96-well microtiter plate (Nalge Nunc International, Rochester, NY) and then the plate was incubated at 37°C without agitation. The plate was removed from the incubator and placed in a Synergy HT plate reader (Bio-Tek Instruments, Winooski, VT) for fluorescence measurements. Excitation and emission wavelengths/slit widths were 450/50 and 485/20 nm,

respectively. Results were plotted using KaleidaGraph, v. 4.0.4 (Synergy Software, Reading, PA).

Neurotoxicity Assay

To determine the effects of Aβ on MTT metabolism, rat pheochromocytoma (PC12) cells were cultured in 75 cm^2 Canted Neck Flasks (Corning Inc., Corning, NY) in F-12K medium containing 10% (v/v) HS, 2.5% (v/v) fetal bovine serum (FBS), 100 units/mL penicillin, 0.1 mg/mL of streptomycin, and 25 µg/mL amphotericin B at 37°C in 5% (v/v) CO_2 in air. The cells were passaged at least 4 times before use. To prepare the PC12 cells for toxicity analysis, the medium was removed and the cells were washed once gently with F-12K medium, containing 0.5% (v/v) FBS, 100 units/mL penicillin, 0.1 mg/mL streptomycin, and 25 µg/mL amphotericin B. A cell suspension was then made with this medium supplemented with 100 µg/mL nerve growth factor (NGF). Cell concentration was determined by Trypan blue staining, after which cells were plated at a concentration of 30,000 cells/well (80 µL of total volume per well) in Costar 96-well white clear-bottom plates (Corning, Corning, NY). The NGF-induced differentiation of the cells was allowed to proceed for 48 h. To perform the toxicity assays, 50 µM of each Aβ assembly was prepared in F-12K medium containing 0.5% (v/v) FBS, 100 units/mL penicillin, 0.1 mg/mL streptomycin, and 25 µg/mL amphotericin B. Twenty µL aliquots of the Aβ solution were added to the wells to yield a final Aβ concentration of 10 µM, which is within the 1-100 µM concentration regime typically used in MTT assays with PC12 cells [18-21]. The cells then were incubated for 17 h, after which 15 µL of CellTiter 96® Non-Radioactive Cell Proliferation Assay MTT solution (Promega, Madison, WI) was added to each well and the plate was incubated at 37°C in the 5% CO2 incubator for 3 h. Thereafter, the cells were lysed by the addition of 100 µL of solubilization solution (Promega, Madison, WI) and the plate was stored overnight at 37°C in 5% CO_2 incubator. The next day, MTT reduction was determined by measuring absorption at 570 nm (corrected for background absorbance at 630 nm) with a Synergy HT plate reader (Bio-Tek

Instruments, Winooski, VT). The negative control was F12-K medium alone. The positive toxicity control was 1 μM staurosporine. Eight to twelve replicates were used for each treatment group and the data were reported as mean ± SE. Percent viability $V = (1 - (A_{A\beta} - A_{medium})/(A_{full\ kill} - A_{medium})) \times 100$, where $A_{A\beta}$, A_{medium}, and $A_{full\ kill}$ were absorbance values from Aβ containing samples, negative control (buffer equivalent with medium), and 1 μM staurosporine alone, respectively.

Cell Culture and Treatment with Aβ

The method of Meberg [22] was used to prepare fresh primary neurons. Embryonic day 18 (E18) rats were sacrificed and the hippocampi were carefully excised using curved forceps. The hippocampi were transferred to Petri dishes, containing 5 mL of Neurobasal A/B27 media (Neurobasal A media supplemented with 2% (v/v) B27), where they were cut into ≈1 mm pieces with a sterilized razor blade. Enzymatic digestion of extracellular matrix proteins was accomplished by trypsin digestion (2 mL of 10× trypsin (2.5% w/v) were added to the suspension for 1h at 37°C in a 5% (v/v) CO_2 incubator). This solution was gently inverted every 5 min. The media was removed and the cells placed in fresh, warm Neurobasal A/B27 media where the cells were dissociated by trituration (20×) with a fire-polished Pasteur pipette. Cell concentrations were quantified using a hemocytometer and 1:1 mixture of a cell culture aliquot:Trypan blue. Cells were plated on Petri dishes or 12-well culture plates previously coated with poly-D-lysine (for at least 2 h) at a concentration of 3×10^5 viable cells/ml. The medium was pre-warmed (37°C) Neurobasal A/B27 media supplemented with 0.5 mM glutamine, 10% (v/v) horse serum (HS), and 10 μg/mL penicillin/streptomycin (P/S). After 2 h incubation in a 37°C, 5% CO_2 incubator, the medium containing unattached cells was removed and fresh medium was added. Cells were allowed to adhere, stabilize metabolically, and grow projections, which typically occurred by 7 days *in vitro* (DIV) (Fig. S1). We note that this protocol has been found to yield almost pure cultures of neurons, although some (<0.5%) glial cells may be

present [23]. Aβ treatment was initiated by removing half the medium and replacing it with an equal volume of fresh medium containing a particular Aβ assembly at a protein concentration of 20 μM. After 24 h, the RNA from these neurons was extracted and used in array analysis.

RNA Extraction, Quantification, and Quality Analysis

Total RNA was obtained using an RNeasy kit (Qiagen, Valencia, CA). The concentration of the RNA in the extracts was determined using a NanoDrop ND-1000 spectrophotometer (Wilmington, DE). The RNA quality was assessed with a RNA Nano 6000 LabChip® (Agilent Technologies, Inc., Santa Clara, CA) and an Agilent 2100 Bioanalyzer (Agilent Technologies, Inc.). Sample RNA integrity number (RIN) was consistently >9 (RIN values above 8 are considered suitable for array analysis) [24].

RNA Amplification, Labeling, and Hybridization

Total RNA was processed at the UCLA Neuroscience Genomics Core (UNGC) and quantified using a Ribogreen fluorescent assay. Intersample RNA concentrations were normalized to 10 ng/μL prior to amplification. Amplified and labeled cRNA was produced using the Illumina-specific Ambion TotalPrep kit based on a T7-based linear amplification method [25]. First and second strand cDNA was produced using the Ambion kit and purified using a robotic assisted magnetic capture step. Briefly, this step employs the use of an oligo(dT) primer coupled to the phage T7 RNA polymerase promoter to prime the synthesis of the complementary DNA by reverse transcription with reverse transcriptase of the poly(A) tail and the associated RNA component of total RNA. Double stranded cDNA (ds cDNA) is produced by RNase H degradation of the original poly A containing RNA followed by strand synthesis with DNA polymerase I. In vitro transcription to synthesize cRNA generates multiple copies of biotinylated cRNA from the double-stranded cDNA templates. Single and double amplification rounds can produce two thousand-fold and one million-fold increases of transcript from the initial

material with typical yields in excess of 1.5 µg. After a second Ribogreen quantification and normalization step, amplified and labeled cRNA was hybridized overnight at 58□C to the RatRef-12 Expression BeadChip (Illumina, San Diego, CA), containing 22,523 probes per array. Hybridization was followed by washing, blocking, staining, and drying on the Little Dipper processor. Array chips were scanned on the Beadarray reader, and expression data was extracted and compiled using BeadStudio software (Illumina).

Microarray Data and Network construction based on WGCNA

The raw data from the microarray was scaled to the same average intensity and normalized using a quantile normalization method [26]. Raw data was analyzed using Bioconductor packages (www.bioconductor.org). Quality was assessed by determining the inter-array Pearson correlation coefficient. Clustering based on top variant genes was used to assess overall data coherence. We performed two distinct analyses: 1) differential expression analysis, and 2) weighted gene co-expression network analysis (WGCNA). Contrast analysis of differential expression was performed using the LIMMA package [27]. After linear model fitting, a Bayesian estimate of differential expression was calculated. Data analysis was aimed at identifying transcriptional changes induced by the various treatments. The threshold for statistical significance was set at $p<0.005$. Gene ontology and pathway analyses were carried out using the "Database for Annotation, Visualization and Integrated Discovery" (https://david.ncifcrf.gov/) and "Ingenuity Pathway Analysis" (www.ingenuity.com). We then conducted WGCNA, a systems biology approach used to identify networks of co-expressed genes in relation to phenotypic data, using the R package, as previously described [28, 29]. Briefly, correlation coefficients were constructed between expression levels of the most variable probes (n=6,274) and a connectivity measure, topological overlap (TO), was calculated for each gene by summing the connection strength with other genes. Genes were then clustered based on their TO,

and groups of co-expressed genes (modules) were identified. Each module was assigned a color, and the first principal component (eigengene) of a module was extracted from the module and considered to be representative of the gene expression profiles in a module [30]. To depict the pairwise relationships between genes, VisANT software (available at http://visant.bu.edu) was employed. Approximately 500 pairs of genes with the highest intra-modular connectivity are shown.

Results

Design and characterization of control peptides

Key factors relevant to the biophysical and biological behavior of Aβ are its: (1) length; (2) pI; (3) amino acid composition; and (4) and sequence. These factors control Aβ assembly (e.g., into oligomers, protofibrils, fibrils) and the interactions between the peptide assemblies and neurons that affect gene expression, cell metabolism, electrical activity, and viability. We reasoned that an ideal control peptide for experiments in which Aβ assembly and biological activity are studied should have the same length, pI, and amino acid composition as the native peptide. Reverse peptides meet this requirement [29, 31-33], but they also maintain identical hydropathy profiles characterized by marked amphipathicity. This means that peptide:neuron interactions involving factors such as partitioning of hydrophobic peptide segments into membranes or formation of membrane pores might be similar for both native and reverse peptides, which would prevent determination of gene expression differences induced by peptide treatment *per se* versus differences linked specifically to Aβ. To eliminate this problem, we designed scrambled Aβ40 (sAβ40) and Aβ42 (sAβ42) sequences having hydropathy profiles with as little divergence as possible from an hydropathy statistic of 0 (Fig. 1; see Methods). We then chemically synthesized sAβ40 and sAβ42 and compared their biophysical properties with those of their cognate native forms to demonstrate that their properties were distinct and thus that the scrambled peptides could indeed be appropriate controls.

Thioflavin T (ThT) fluorescence

Temporal changes in Thioflavin T (ThT) fluorescence were used to reveal β-sheet formation for freshly prepared, aggregate-free Aβ incubated at 37°C. Aβ40 displayed a monotonic increase in ThT fluorescence that reached a plateau after ≈200 h (Fig. 2A, black circles). The ThT signal increased 15-fold during the assay, demonstrating that β-sheet formation occurred. In comparison, sAβ40 showed a relatively small (2-fold) increase in ThT fluorescence that reached a plateau after ≈60 h (Fig. 2A, white circles). Aβ42 displayed a rapid increase in ThT fluorescence that reached a plateau of ≈520 FU after ≈50 h (Fig. 2B, black circles). In comparison, sAβ42 showed a rapid, transient increase in ThT fluorescence within 10 h that decreased to, and remained at, baseline levels (≈30-40 FU) after ≈50 h (Fig. 2B, white circles).

Circular dichroism (CD) spectroscopy

We used CD spectroscopy to determine secondary structure dynamics. Aβ40 initially displayed a spectrum characterized by a prominent minimum at ≈198 nm and increasing ellipticity toward higher wavelengths (Fig. 3A). Inflections were observed at ≈215 and ≈230 nm. This spectrum is characteristic of statistical coil secondary structure [34, 35]. The spectral shape changed progressively during 14 d of incubation, yielding a final spectrum displayed a peak of ellipticity at ≈195 nm and a minimum at ≈215 nm, consistent with β-sheet. In contrast, sAβ40 displayed spectra consistent with statistical coil throughout the incubation period (Fig. 3B). Qualitatively similar data were observed in studies of Aβ42. The initial Aβ42 spectrum displayed statistical coil characteristics, which changed over time to a classical β-sheet form (Fig. 3C). SAβ42 displayed spectra consistent with statistical coil secondary structure throughout the incubation period (Fig. 3D).

Oligomerization

The oligomerization of the different Aβ peptides was monitored by zero-length, photochemical cross-linking (PICUP) followed by SDS-PAGE and silver staining (Fig. 4). In the absence of cross-linking, Aβ40 displayed almost exclusively monomers (Fig. 4, lane 1). After cross-linking, the Aβ40 oligomer distribution comprised monomers through hexamers (Fig. 4, lane 2), with trimer exhibiting the most intense band. Aβ42 displayed monomers and trimers (Fig. 4, lane 3). After cross-linking, Aβ42 produced an oligomer distribution comprising monomers through octamers (Fig. 4, lane 4), with nodes at dimer and pentamer/hexamer (Fig. 4, black arrowhead). SAβ40 displayed monomers, but no higher molecular weight bands (Fig. 4, lane 5). Four prominent bands were observed after cross-linking of sAβ40, which we interpret to be dimer through pentamer (Fig. 4, lane 6). A faint hexamer band also was seen. A similar pattern of bands was seen with sAβ42 (Fig. 4, lane 8). We note that the mobilities of the bands in the two cross-linked scrambled peptides differed from the mobilities of the respective bands in the wild type Aβ40 (cf. lanes 2 and 6) and Aβ42 samples (cf. lanes 4 and 8). We note, in addition, that the cross-linking of the scrambled peptides was particularly efficient relative to the wild type peptides (cf. monomer band intensities of lanes 5 and 7 with those of lanes 6 and 8; and monomer intensities of lanes 1 and 3 with those of lanes 2 and 4). Taken together with the results of the CD experiments, these data suggest that the scrambled peptides interact rapidly to form oligomers but that these oligomers do not possess the ordered secondary structure elements (e.g., β-sheet) found in Aβ40 and Aβ42.

Toxicity

To study the biological activity of the scrambled peptides and how it related to the activities of LMW, oligomeric (oligomers stabilized by cross-linking; XL), and fibrillar Aβ assemblies, we studied the effects of the different Aβ preparations on cell metabolism using MTT assays [36]. To do so, rat

pheochromocytoma (PC12) cells were treated with sAβ, LMW Aβ, cross-linked Aβ, or fibrillar Aβ for 24 h at 37°C and then the ability of the cells to metabolize MTT was measured (Fig. 5). The metabolic activity of cells treated with LMW Aβ40 and LMW Aβ42 was 73% and 83% of the buffer control, respectively, demonstrating modest cytotoxic activity for these Aβ assemblies. Cross-linked Aβ40 and Aβ42 produced similar toxic effects. Fibrils of Aβ40 and Aβ42 were significantly more toxic, reducing MTT metabolism by 63% and 45%, respectively. Only the SAβ40- and sAβ42-treated cells displayed no significant metabolic effects. It has been reported that oligomeric forms of Aβ are more toxic than fibrils [13]. The most likely explanation for the modest toxicity displayed by the oligomers used here is that their structures differ from those used by Dahlgren *et al.*, which were not stabilized by covalent cross-linking.

Effects of Aβ assemblies on neuronal gene expression

Our goal in designing sAβ40 and sAβ42 was to control experiments determining structure-activity relationships. The prior results showed that these peptides did not share fibril formation (ThT) or secondary structure (CD) dynamics, oligomerization patterns, or neurotoxic activity (MTT) with their wild type analogues, demonstrating achievement of the goal. We thus used these peptide to control experiments monitoring changes in neuronal gene expression induced by exposure of rat primary Hc neurons to: (1) LMW Aβ (predominately monomers and dimers); (2) low-order, stable, Aβ oligomers; or (3) Aβ fibrils. These species represent three major classes of Aβ assemblies with potential relevance to AD [7]. Primary rat Hc neurons were incubated for 24 h with each of four different types of Aβ40 or Aβ42 peptides—LMW, cross-linked oligomers, fibrillar, or scrambled. RNA then was harvested from each treatment group and hybridized onto rat microarray chips. First, analysis of average signal intensity differences among genes allowed us to make comparisons between different treatment groups (Fig. 6, Table S1). The largest numbers of gene changes occurred with fibril treatment,

consistent with the relatively large toxicity of fibrils observed in the MTT assays groups. The total number of changes observed in the fibril-treated groups varied from ≈1050-1600, with similar (±10%) numbers of genes on average showing increased and decreased expression. The largest overall gene expression changes were seen in Aβ42 fibrils vs. control-treated neurons, where 860 and 735 genes are under- and over-expressed, respectively. In comparison, Aβ42 fibrils vs. sAβ42-treated neurons showed 671 and 663 genes under- and over-expressed, respectively. The relative difference in differential gene expression between these two groups may be explained in part by sAβ42 alone, which results in under- and over-expression of 47 and 59 genes, respectively.

We also observed a large number of gene expression changes for cross-linked Aβ40, which demonstrated ~400 gene changes versus sAβ40. One interesting feature of the dataset was the relatively low number of changes observed with cross-linked Aβ42 compared to the numbers observed with both Aβ40 and Aβ42 fibrils or cross-linked Aβ40. Clustering based on the overall differences in gene expression revealed that neurons treated with fibrillar Aβ cluster separately from other treatment groups (Fig. 7A). Furthermore, neurons treated with cross-linked Aβ40 clustered separately from all other treatment groups. In general, the dendrogram branching pattern suggests that the treatment groups with the greatest magnitude of gene changes cluster separately from those with fewer than 400 gene changes.

Gene ontology analysis of the top differentially expressed genes observed in cells treated with Aβ42 fibrils vs. sAβ42 revealed overrepresentation of transcripts generally related to inflammatory response (including response to stimulus and other organism), regulation of cell proliferation, and programmed cell death (Figure 7B). Transcripts included in these categories were mostly up regulated, supporting the notion that treatment with some Aβ assemblies induces an inflammatory response in cultured neurons, which can be associated with cell death.

Network construction and modular organization

Next, we performed weighted gene co-expression network analysis (WGCNA) [29] to elucidate the complex, high-order relationships among gene expression levels. Networks were constructed based on gene topological overlap (TO), which considers the level of correlation between two genes and their degree of shared correlation within the network [29].

Seven thousand of the most variable genes were clustered using TO as a similarity metric, where similarly co-expressed probes clustered together. Distinct groups of clustered genes, termed "modules", were then defined using an algorithm that analyzes branching pattern [30], and a color was assigned to each module (Fig. S2). We then correlated for each module the module eigengene (ME), a weighted summation of expression profiles of all the transcripts in a given module [37], with the presence or absence of Aβ treatment. The orange and yellow modules, which are independent from one another, showed the greatest correlation with Aβ40 and Aβ42 fibril treatment among the total of 13 modules defined. As expected, in each of these modules, the largest number of gene expression changes was seen for neurons treated with fibrillar Aβ40 or fibrillar Aβ42 (see Fig. 6). However, each module had distinct gene ontologies. The orange module showed an overrepresentation of genes involved in extracellular matrix formation and the yellow module an overrepresentation of transcripts involved in inflammation and responses to cytokines.

The network position of a particular gene was then determined by calculating the ME-centered connectivity. Those transcripts with the highest levels of connectivity (i.e., correlation with the ME) were designated as hub genes. Top hub probes for the orange module included *Ogn*, *LOC311722*, *LOC498662*, *Lox*, *MGC72614*, and *Bambi* (Fig. 8). *Ogn* is the gene for the proteoglycan osteoglycan. *LOC311722*, *LOC498662*, and *MGC72614* are yet uncharacterized genes. *Lox* encodes lysyl oxidase, which is an extracellular copper enzyme that catalyzes the cross-linking of structural proteins such as collagen and elastin. Bambi is transmembrane glycoprotein known to negatively regulate

transforming growth factor-β [38]. Network visualization of the yellow module reveals six hub genes: *LOC497812*, *Isg12(b)*, *Ifit1*, *RT1-Da*, *Cxcl11*, and *Rtp4*. (Fig. 9). LOC497812 is an uncharacterized gene. *Isg12(b)*, *Ifit1*, and *Rtp4* are proteins responsive to interferon-γ (IFN-γ). *RT1-Da* is a major histocompatibility (MHC) class II molecule. *Cxcl11* is an inflammatory cytokine.

Discussion

We have hypothesized that a central etiologic mechanism of AD is age-dependent alteration in neuronal gene expression in response to specific Aβ assemblies. To test this hypothesis, it was necessary to control gene expression experiments for effects caused simply by the interaction of peptides *per se* with neurons, as distinguished from effects induced by particular Aβ conformers or assemblies (monomers, oligomers, protofibrils, or fibrils). First principles argued that an ideal control would have an amino acid composition identical to that of the native peptide, and therefore identical molecular weight, length, and pI, but *not* share conformational features or assembly properties. We have shown, using a combination of Kyte-Doolittle analysis, ThT fluorescence, CD, photochemical cross-linking and SDS-PAGE/silver staining, and MTT assays, that the scrambled peptides sAβ40 and sAβ42 did not share hydropathy profiles, conformational dynamics, assembly kinetics, or neurotoxic activity with their cognate wild type peptides. These data validated the use of the scrambled peptides as controls, enabling us to begin testing our hypothesis about Aβ-assembly dependent effects on neuronal gene expression.[1]

[1] We are aware of two other sequences of scrambled Aβ40 and Aβ42 (available from commercial sources (Table S2)). Class I peptides have been used in studies of Aβ-induced expression of BACE1 mRNA in primary neuronal cultures [39], intracellular rod formation in primary hippocampal neurons [40], ligand blotting to APP [41], and clearance of Aβ through the blood-brain barrier [42]. Class II peptides have

We began first by studying the effects of Aβ monomers and dimers, oligomers, and fibrils on gene expression using embryonic rat primary Hc neurons. We did so to establish how Aβ assembly types thought to be important in disease causation affected "young" neurons. These studies are a necessary prerequisite for later work using adult neurons. Our analysis revealed a gradient of gene expression changes induced by specific Aβ assemblies, with the largest magnitude of changes induced by Aβ40 and Aβ42 fibril treatment. The dominant ontology categories affected by these treatments are related to activation of inflammatory pathways. WGCNA also identified two co-expression modules correlated with Aβ40 and Aβ42 fibril treatment that were related to extracellular matrix and inflammation. These results are consistent with recent reports that transforming growth factor-β1 blocks CCL5, which is a chemokine that mediates the chemotaxis of microglia towards Aβ aggregates [44], and that increased expression of argininosuccinate synthetase (the rate-limiting enzyme in the metabolic pathway for the conversion of L-citrulline to L-arginine, which is a substrate for all isoforms of nitric oxide synthases (NOS) [45]) and inducible NOS (iNOS) is observed in the cortices of AD patients [46]. NO appears to play a key role in inflammatory processes in the CNS, including both neurotoxic and protective [47]. In rat mixed neuronal-glial cultures, Aβ induced the expression of iNOS and argininosuccinate synthetase with a corresponding increase in inflammatory cytokines such as interleukin-1β and tumor necrosis factor-α [46]. The observation of

---

been used in studies of astrocyte activation [43]. No systematic studies of the structures and assembly dynamics of these two classes of peptides were reported. EM studies did show that class I scrambled Aβ40 and Aβ42 did not form "appreciable high molecular weight aggregates" after 1 or 6h when examined by EM [39] and CD spectra obtained immediately after preparation of class II scrambled [Iodo-tyrosyl10]Aβ40 were identical to those obtained from wild type [Iodo-tyrosyl10]Aβ40 [42]. Aggregates were formed by class II scrambled Aβ42 and these aggregates caused modest astrocyte activation [43].

significant cytokine expression is especially interesting in light of recent evidence that the chemokine CX_3CL1 (fractalkine) is implicated in the progression and severity of AD-like pathology in mice [48, 49] and that knockout of its receptor CX_3CR1 protects against Aβ-induced neurotoxicity in rodents [50].

Acknowledgements

We gratefully acknowledge Margaret Condron for synthesizing and purifying the peptides used in this study and Fuying Gao for assistance with microarray data processing.

Supporting Information Available

Table S1, Average signal intensity differences among genes after treatment with specific Aβ assemblies; **Table S2,** Commercially available scrambled Aβ peptides; **Fig. S1,** Phase-contrast microscopy image of primary hippocampal neurons after 7 days in culture; **Fig. S2,** Relationship between module eigengene (first principal component, corresponding to the weighted summation of expression across all the probes included in a given module) and treatment (Aβ assembly type).

Funding Information

This project was supported by the UCLA Medical Scientist Training Program (MSTP) (GY), the UCLA Chemistry-Biology Interface (CBI) Training Program (GY), the UCSD Clinician Scientist Program (#5T32EB005970-07) (GY), NIH Grants NS038328 (DBT) and AG041295 (DBT), the Jim Easton Consortium for Drug Discovery and Biomarkers at UCLA (DBT), and the NINDS Informatics Center for Neurogenetics and Neurogenomics (P30 NS062691).

Figure Legends

Figure 1. Hydropathy profiles for Aβ42, reverse Aβ42 (rAβ42), and scrambled Aβ42 (sAβ42). Abscissa shows position of center of hydropathy window of 9 amino acids. Ordinate is hydropathy metric that denotes hydrophobicity as positive and hydrophilicity as negative.

Figure 2. Time-dependence of ThT fluorescence. (A) Aβ40 (black circles) and sAβ40 (white circles) were incubated at 37 °C and Thioflavin T (ThT) fluorescence was determined periodically. (B) Aβ42 (black circles) and sAβ42 (white circles) was studied in an identical manner. Fluorescence is presented in arbitrary units (FU). Curve fits are included only for ease of comparison between curves. A minimum of three replicates was done for each sample.

Figure 3. Circular dichroism spectroscopy. Secondary structure dynamics of WT vs. sAβ were determined using CD. Spectra are: (A) Aβ40, (B) sAβ40, (C) Aβ42, and (D) sAβ42. Spectra were acquired at times: 0 h (white circles), 24 h (black circles), 120 h (white triangles), 240 h (black triangles), and 340 h (white squares). A minimum of three replicates was done for each sample.

Figure 4. Oligomer size distributions. PICUP, SDS-PAGE, and silver staining were used to determine the oligomer size distribution of freshly prepared Aβ40, Aβ42, sAβ40, and sAβ42. Lane 1, non-cross-linked Aβ40; Lane 2, cross-linked Aβ40; Lane 3, non-cross-linked Aβ42; Lane 4, cross-linked Aβ42; Lane 5, non-cross-linked sAβ40; Lane 6, cross-linked sAβ40; Lane 7, non-cross-linked sAβ42; Lane 8, cross-linked sAβ42. The results are representative of those obtained in each of three independent experiments. Numbers to the right of lanes signify oligomer order (number of monomers). Black arrowhead indicates an intensity node at pentamer/hexamer.

Figure 5. Toxicity of different Aβ assemblies. MTT assays were performed on differentiated PC12 cells using 10 μM final concentrations of LMW Aβ40, LMW Aβ42, cross-linked Aβ40, cross-linked Aβ42, fibrillar Aβ40, fibrillar Aβ42, sAβ40, and sAβ42. Standard errors were derived from 8-12 repetitions of each experiment. Toxicity measurements were normalized to buffer control. The statistical signifance of the differences between the mean of LMW Aβ40 and the means of XL Aβ40 oligomers, Aβ40 fibrils, or scrambled Aβ40 is indicated by p-values, as follows: *, p<0.05; **, p<.005, and p<0.0005. p-values for XL Aβ42 oligomers, Aβ42 fibrils, or scrambled Aβ42 are represented by the same symbols but were calculated relative to the mean of LMW Aβ42. ND means "not done," and NS means "not significant."

Figure 6: Bar plot representing the number of down regulated (green) and up regulated (red) genes in each comparison. Complete gene lists are in Table S1.

Figure 7: (A) Heat map depicting gene expression changes at each of the comparisons ($p < 0.005$, Bayesian *t*-test). Each row corresponds to one probe, and each column corresponds to one comparison. Up regulated genes are in red and down regulated genes are in green. The color intensity corresponds to the magnitude of the change in expression level (probes are listed in Supplementary Table). Both comparisons and probes are clustered by similarity (represented by the cluster dendrograms on top and side, respectively). Comparisons are numbered as follows: 1) LMW Aβ42 vs. sAβ42; 2) LMW Aβ40 vs. sAβ40; 3) cross-linked Aβ42 vs. sAβ42; 4) cross-linked Aβ40 vs. sAβ40; 5) Aβ40 fibrils vs. sAβ40; 6) Aβ42 fibrils vs. sAβ42. (B) Over-represented gene ontology (GO) categories among differentially expressed genes in Aβ42 fibrils vs. sAβ42 (the proportion of down regulated DE genes is in green and the proportion of up regulated DE genes is in red) sorted by –log10 (*p* value). A –log (*p* value) of 1.3 corresponds to an over-representation *p* value of 0.05.

Figure 8. Network visualization of the orange module. This plot represents the strongest connections, based on topological overlap (TO), within the orange module and highlights the central most connected genes, or hubs, within the network. The hub genes, which are highlighted with red circles, are Ogn, LOC311722, LOC498662, Lox, MGC72614, and Bambi.

Figure 9. Network visualization of the yellow module. This plot represents the strongest connections, based on TO, within the yellow module and highlights the central most connected genes, or hubs, within the network. The hub genes, which are highlighted with red circles, are LOC497812, Isg12(b), Ifit1, RT1-Da, Cxcl11, and Rtp4.

References

[1] Goedert, M., and Spillantini, M. G. (2006) A century of Alzheimer's disease, *Science 314*, 777-781.

[2] Brookmeyer, R., Johnson, E., Ziegler-Graham, K., and Arrighi, H. M. (2007) Forecasting the global burden of Alzheimer's disease., *Alzheimers Dement 3*, 186-191.

[3] Selkoe, D. J. (2001) Alzheimer's disease: genes, proteins, and therapy, *Physiol Rev 81*, 741-766.

[4] Pillot, T., Drouet, B., Queille, S., Labeur, C., Vandekerckhove, J., Rosseneu, M., Pincon-Raymond, M., and Chambaz, J. (1999) The nonfibrillar amyloid β-peptide induces apoptotic neuronal cell death: Involvement of its C-terminal fusogenic domain, *J Neurochem 73*, 1626-1634.

[5] Suo, Z. M., Humphrey, J., Kundtz, A., Sethi, F., Placzek, A., Crawford, F., and Mullan, M. (1998) Soluble Alzheimers β-amyloid constricts the cerebral vasculature in vivo, *Neurosci Lett 257*, 77-80.

[6] Selkoe, D. J. (1991) The molecular pathology of Alzheimer's disease, *Neuron 6*, 487-498.

[7] Roychaudhuri, R., Yang, M., Hoshi, M. M., and Teplow, D. B. (2009) Amyloid β-protein assembly and Alzheimer disease, *J Biol Chem 284*, 4749-4753.

[8] Walsh, D. M., and Selkoe, D. J. (2007) Aβ oligomers - a decade of discovery, *J Neurochem 101*, 1172-1184.

[9] Hayden, E. Y., and Teplow, D. B. (2013) Amyloid β-protein oligomers and Alzheimer's disease, *Alzheimers Res Ther 5*, 60.

[10] Kyte, J., and Doolittle, R. F. (1982) A simple method for displaying the hydropathic character of a protein, *J Mol Biol 157*, 105-132.

[11] Walsh, D. M., Hartley, D. M., Kusumoto, Y., Fezoui, Y., Condron, M. M., Lomakin, A., Benedek, G. B., Selkoe, D. J., and Teplow, D. B. (1999) Amyloid β-protein fibrillogenesis. Structure and

biological activity of protofibrillar intermediates, *J Biol Chem 274*, 25945-25952.

[12] Bitan, G., Kirkitadze, M. D., Lomakin, A., Vollers, S. S., Benedek, G. B., and Teplow, D. B. (2003) Amyloid β-protein (Aβ) assembly: Aβ40 and Aβ42 oligomerize through distinct pathways, *Proc Natl Acad Sci U S A 100*, 330-335.

[13] Dahlgren, K. N., Manelli, A. M., Stine, W. B., Jr., Baker, L. K., Krafft, G. A., and LaDu, M. J. (2002) Oligomeric and fibrillar species of amyloid-β peptides differentially affect neuronal viability, *J Biol Chem 277*, 32046-32053.

[14] Lambert, M. P., Barlow, A. K., Chromy, B. A., Edwards, C., Freed, R., Liosatos, M., Morgan, T. E., Rozovsky, I., Trommer, B., Viola, K. L., Wals, P., Zhang, C., Finch, C. E., Krafft, G. A., and Klein, W. L. (1998) Diffusible, nonfibrillar ligands derived from $A\beta_{1-42}$ are potent central nervous system neurotoxins, *Proc Natl Acad Sci U S A 95*, 6448-6453.

[15] Lesné, S., Koh, M. T., Kotilinek, L., Kayed, R., Glabe, C. G., Yang, A., Gallagher, M., and Ashe, K. H. (2006) A specific amyloid-β protein assembly in the brain impairs memory, *Nature 440*, 352-357.

[16] Gellermann, G. P., Byrnes, H., Striebinger, A., Ullrich, K., Mueller, R., Hillen, H., and Barghorn, S. (2008) Aβ-globulomers are formed independently of the fibril pathway, *Neurobiol Dis 30*, 212-220.

[17] Hoshi, M., Sato, M., Matsumoto, S., Noguchi, A., Yasutake, K., Yoshida, N., and Sato, K. (2003) Spherical aggregates of β-amyloid (amylospheroid) show high neurotoxicity and activate tau protein kinase I/glycogen synthase kinase-3β, *Proc Natl Acad Sci U S A 100*, 6370-6375.

[18] Muthaiyah, B., Essa, M. M., Chauhan, V., and Chauhan, A. (2011) Protective effects of walnut extract against amyloid beta peptide-induced cell death and oxidative stress in PC12 cells, *Neurochem Res 36*, 2096-2103.

[19] Zhi-Kun, S., Hong-Qi, Y., Zhi-Quan, W., Jing, P., Zhen, H., and Sheng-Di, C. (2012) Erythropoietin prevents PC12 cells from beta-amyloid-induced apoptosis via PI3KAkt pathway, *Transl*

Neurodegener 1, 7.

[20] McKoy, A. F., Chen, J., Schupbach, T., and Hecht, M. H. (2014) Structure-activity relationships for a series of compounds that inhibit aggregation of the Alzheimer's peptide, Aβ42, *Chem Biol Drug Des 84*, 505-512.

[21] Simakova, O., and Arispe, N. J. (2007) The cell-selective neurotoxicity of the Alzheimer's Aβ peptide is determined by surface phosphatidylserine and cytosolic ATP levels. Membrane binding is required for Aβ toxicity, *J Neurosci 27*, 13719-13729.

[22] Meberg, P. J., and Miller, M. W. (2003) Culturing hippocampal and cortical neurons, In *Methods in Cell Biology* (Hollenbeck, P. J. a. B., James R., Ed.), pp 111-127, Elsevier Science (USA), San Diego.

[23] Brewer, G. J., Torricelli, J. R., Evege, E. K., and Price, P. J. (1993) Optimized survival of hippocampal neurons in B27-supplemented neurobasal™, a new serum-free medium combination, *J Neurosci Res 35*, 567-576.

[24] Schroeder, A., Mueller, O., Stocker, S., Salowsky, R., Leiber, M., Gassmann, M., Lightfoot, S., Menzel, W., Granzow, M., and Ragg, T. (2006) The RIN: an RNA integrity number for assigning integrity values to RNA measurements, *BMC Mol Biol 7*, 3.

[25] Van Gelder, R. N., von Zastrow, M. E., Yool, A., Dement, W. C., Barchas, J. D., and Eberwine, J. H. (1990) Amplified RNA synthesized from limited quantities of heterogeneous cDNA, *Proc Natl Acad Sci U S A 87*, 1663-1667.

[26] Coppola, G., Karydas, A., Rademakers, R., Wang, Q., Baker, M., Hutton, M., Miller, B. L., and Geschwind, D. H. (2008) Gene expression study on peripheral blood identifies progranulin mutations, *Ann Neurol 64*, 92-96.

[27] Smyth, G. K. (2005) Limma: Linear models for microarray data, In *Bioinformatics and Computational Biology Solutions Using R and Bioconductor* (R. Gentleman, V. C., S. Dudoit, R.

Irizarry, and W. Huber, Ed.), pp 397–420, Springer, New York.

[28] Langfelder, P., and Horvath, S. (2008) WGCNA: an R package for weighted correlation network analysis, *BMC Bioinformatics 9*, 559.

[29] Zhang, B., and Horvath, S. (2005) A general framework for weighted gene co-expression network analysis, *Stat Appl Genet Mol Biol 4*, Article17.

[30] Langfelder, P., Zhang, B., and Horvath, S. (2008) Defining clusters from a hierarchical cluster tree: the Dynamic Tree Cut package for R, *Bioinformatics 24*, 719-720.

[31] Bruban, J., Glotin, A. L., Dinet, V., Chalour, N., Sennlaub, F., Jonet, L., An, N., Faussat, A. M., and Mascarelli, F. (2009) Amyloid-β(1-42) alters structure and function of retinal pigmented epithelial cells, *Aging Cell 8*, 162-177.

[32] Fraser, P. E., Nguyen, J. T., Inouye, H., Surewicz, W. K., Selkoe, D. J., Podlisny, M. B., and Kirschner, D. A. (1992) Fibril formation by primate, rodent, and Dutch-hemorrhagic analogues of Alzheimer amyloid β-protein, *Biochemistry 31*, 10716-10723.

[33] Parameshwaran, K., Sims, C., Kanju, P., Vaithianathan, T., Shonesy, B. C., Dhanasekaran, M., Bahr, B. A., and Suppiramaniam, V. (2007) Amyloid beta-peptide $A\beta_{1-42}$ but not $A\beta_{1-40}$ attenuates synaptic AMPA receptor function, *Synapse 61*, 367-374.

[34] Drake, A. F. (1994) Circular dichroism, *Methods Mol Biol 22*, 219-244.

[35] Fasman, G. D. (1996) *Circular dichroism and the conformational analysis of biomolecules*, Plenum Press, New York.

[36] Datki, Z., Juhasz, A., Galfi, M., Soos, K., Papp, R., Zadori, D., and Penke, B. (2003) Method for measuring neurotoxicity of aggregating polypeptides with the MTT assay on differentiated neuroblastoma cells, *Brain Res Bull 62*, 223-229.

[37] Oldham, M. C., Konopka, G., Iwamoto, K., Langfelder, P., Kato, T., Horvath, S., and Geschwind, D. H. (2008) Functional organization of the transcriptome in human brain, *Nat Neurosci 11*, 1271-

1282.

[38] Tramullas, M., Lantero, A., Diaz, A., Morchon, N., Merino, D., Villar, A., Buscher, D., Merino, R., Hurle, J. M., Izpisua-Belmonte, J. C., and Hurle, M. A. (2010) BAMBI (bone morphogenetic protein and activin membrane-bound inhibitor) reveals the involvement of the transforming growth factor-β family in pain modulation, *J Neurosci 30*, 1502-1511.

[39] Giliberto, L., Borghi, R., Piccini, A., Mangerini, R., Sorbi, S., Cirmena, G., Garuti, A., Ghetti, B., Tagliavini, F., Mughal, M. R., Mattson, M. P., Zhu, X., Wang, X., Guglielmotto, M., Tamagno, E., and Tabaton, M. (2009) Mutant presenilin 1 increases the expression and activity of BACE1, *J Biol Chem 284*, 9027-9038.

[40] Maloney, M. T., Minamide, L. S., Kinley, A. W., Boyle, J. A., and Bamburg, J. R. (2005) β-secretase-cleaved amyloid precursor protein accumulates at actin inclusions induced in neurons by stress or amyloid β: a feedforward mechanism for Alzheimer's disease, *J Neurosci 25*, 11313-11321.

[41] Shaked, G. M., Kummer, M. P., Lu, D. C., Galvan, V., Bredesen, D. E., and Koo, E. H. (2006) Aβ induces cell death by direct interaction with its cognate extracellular domain on APP (APP 597-624), *FASEB J 20*, E546-E555.

[42] Ji, Y., Permanne, B., Sigurdsson, E. M., Holtzman, D. M., and Wisniewski, T. (2001) Amyloid β40/42 clearance across the blood-brain barrier following intra-ventricular injections in wild-type, apoE knock-out and human apoE3 or E4 expressing transgenic mice, *J Alzheimers Dis 3*, 23-30.

[43] Hu, J., Akama, K. T., Krafft, G. A., Chromy, B. A., and Van Eldik, L. J. (1998) Amyloid-β peptide activates cultured astrocytes: morphological alterations, cytokine induction and nitric oxide release, *Brain Res 785*, 195-206.

[44] Huang, W. C., Yen, F. C., Shie, F. S., Pan, C. M., Shiao, Y. J., Yang, C. N., Huang, F. L., Sung, Y. J., and Tsay, H. J. (2010) TGF-β1 blockade of microglial chemotaxis toward Aβ aggregates involves SMAD signaling and down-regulation of CCL5, *J Neuroinflammation 7*, 28.

[45] Heneka, M. T., Wiesinger, H., Dumitrescu-Ozimek, L., Riederer, P., Feinstein, D. L., and Klockgether, T. (2001) Neuronal and glial coexpression of argininosuccinate synthetase and inducible nitric oxide synthase in Alzheimer disease, *J Neuropathol Exp Neurol 60*, 906-916.

[46] Haas, J., Storch-Hagenlocher, B., Biessmann, A., and Wildemann, B. (2002) Inducible nitric oxide synthase and argininosuccinate synthetase: co-induction in brain tissue of patients with Alzheimer's dementia and following stimulation with β-amyloid 1-42 in vitro, *Neurosci Lett 322*, 121-125.

[47] Calabrese, V., Mancuso, C., Calvani, M., Rizzarelli, E., Butterfield, D. A., and Stella, A. M. (2007) Nitric oxide in the central nervous system: neuroprotection versus neurotoxicity, *Nat Rev Neurosci 8*, 766-775.

[48] Chapman, G. A., Moores, K., Harrison, D., Campbell, C. A., Stewart, B. R., and Strijbos, P. J. (2000) Fractalkine cleavage from neuronal membranes represents an acute event in the inflammatory response to excitotoxic brain damage, *J Neurosci 20*, RC87.

[49] Wu, J., Bie, B., Yang, H., Xu, J. J., Brown, D. L., and Naguib, M. (2013) Suppression of central chemokine fractalkine receptor signaling alleviates amyloid-induced memory deficiency, *Neurobiol Aging 34*, 2843-2852.

[50] Dworzak, J., Renvoise, B., Habchi, J., Yates, E. V., Combadiere, C., Knowles, T. P., Dobson, C. M., Blackstone, C., Paulsen, O., and Murphy, P. M. (2015) Neuronal Cx3cr1 Deficiency Protects against Amyloid β-Induced Neurotoxicity, *PLoS One 10*, e0127730.

Fig. 1

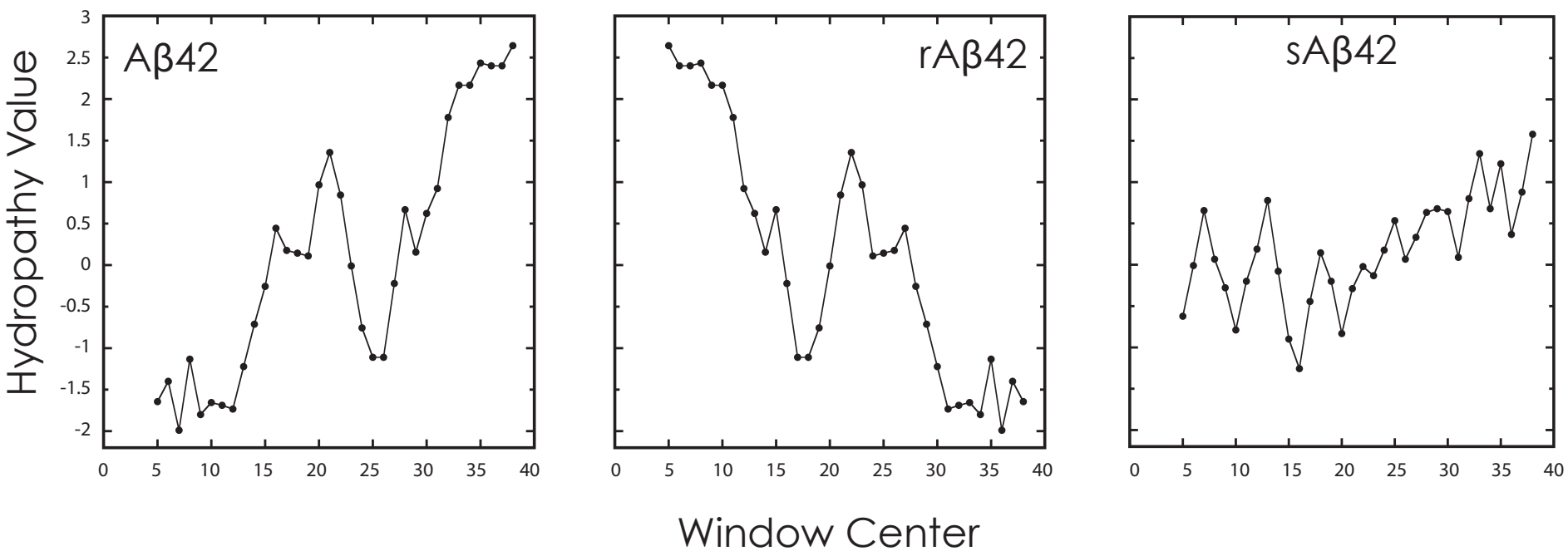
Aβ42
rAβ42
sAβ42
Hydropathy Value
Window Center
3
2.5
2
1.5
1
0.5
0
-0.5
-1
-1.5
-2
0
5
10
15
20
25
30
35
40

Fig. 2A

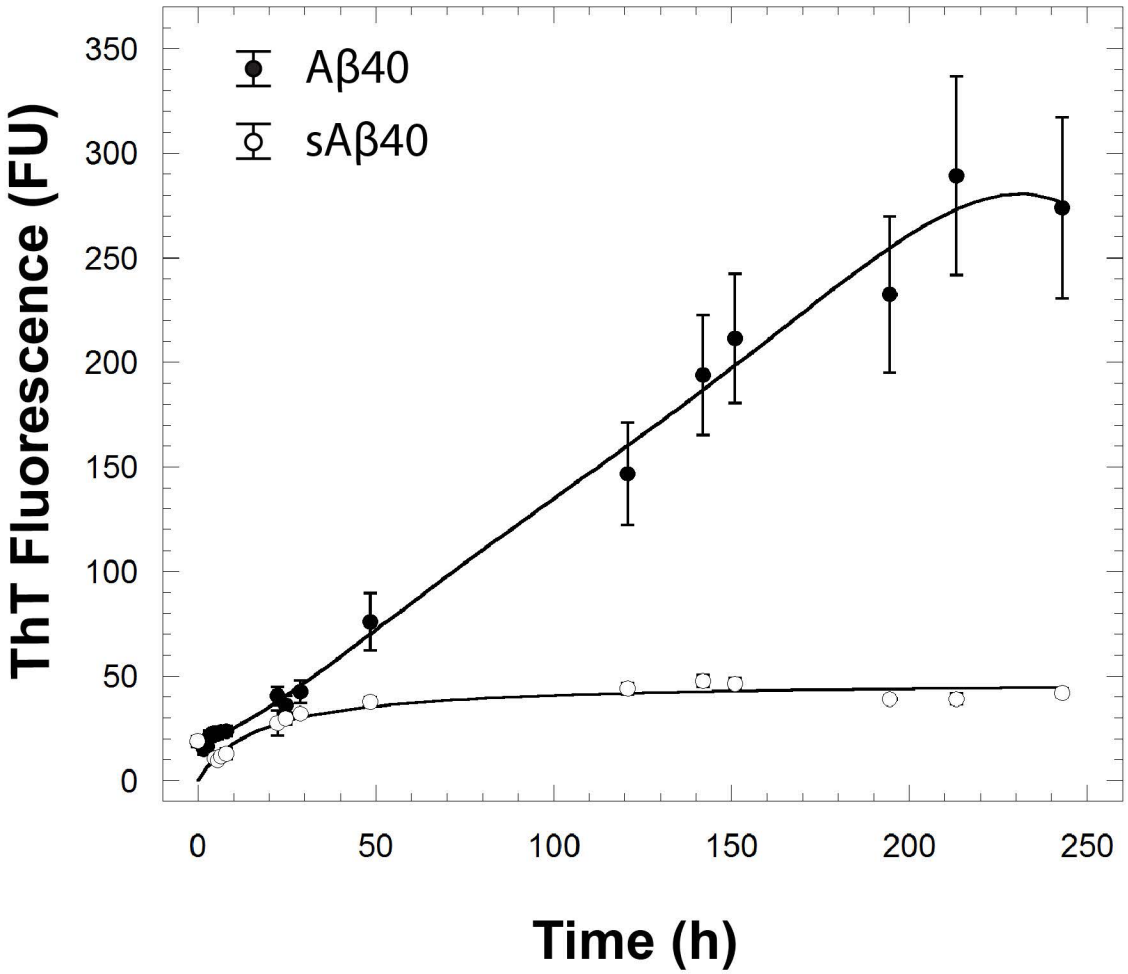
Aβ40
sAβ40
ThT Fluorescence (FU)
Time (h)
0
50
100
150
200
250
300
350

Fig. 2B

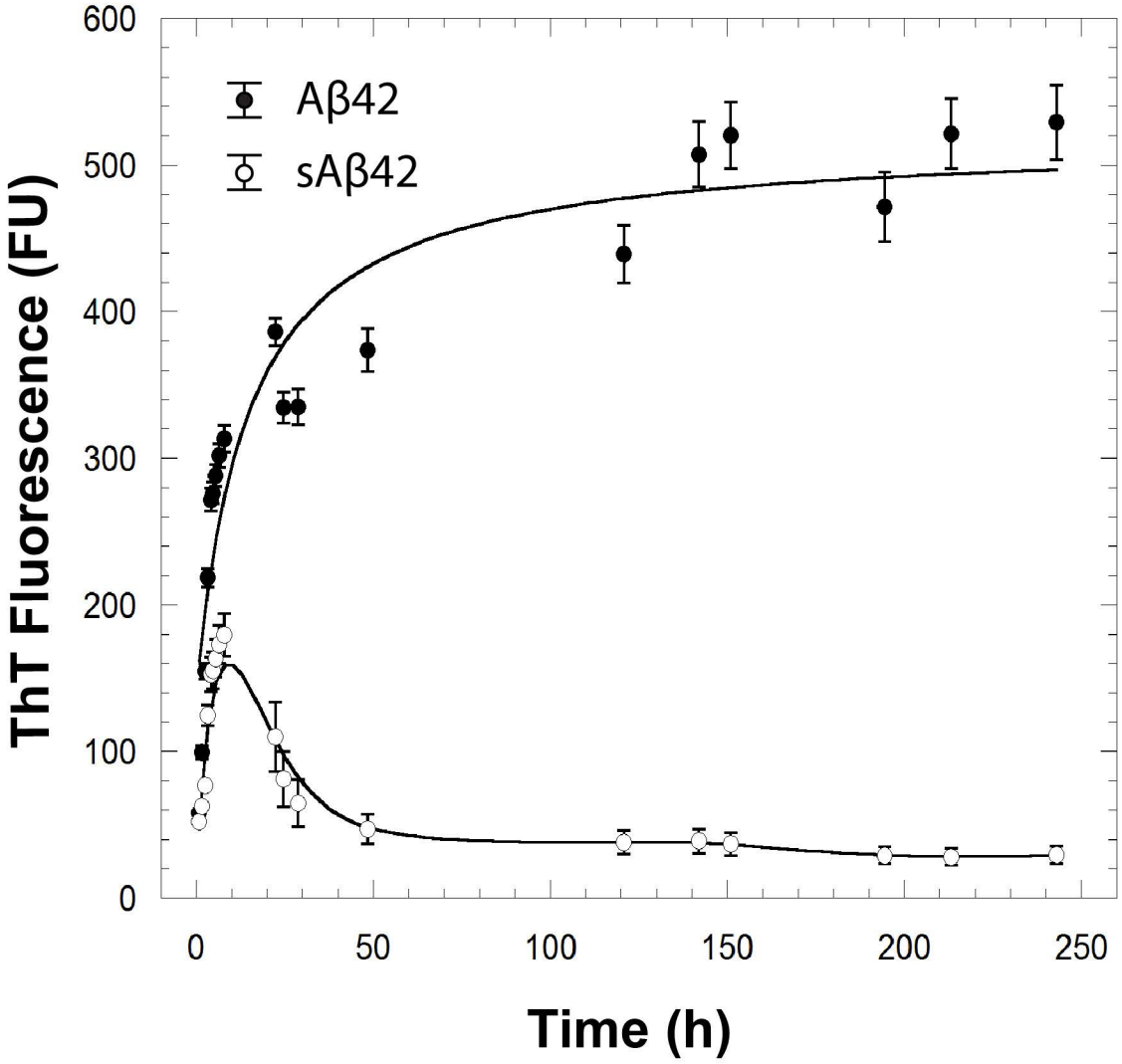
Aβ42
sAβ42
ThT Fluorescence (FU)
Time (h)
0
100
200
300
400
500
600
0
50
100
150
200
250

Fig. 3

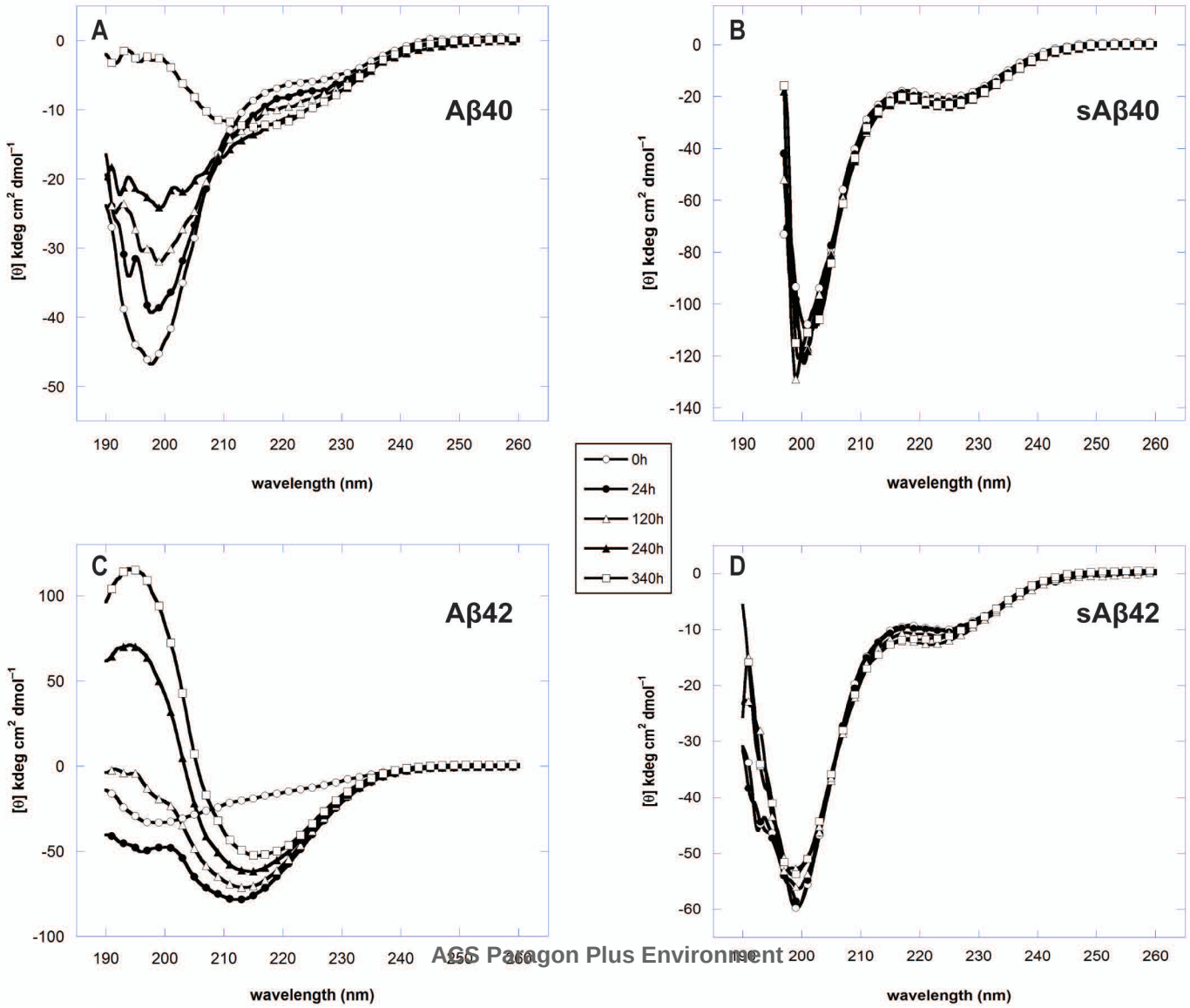

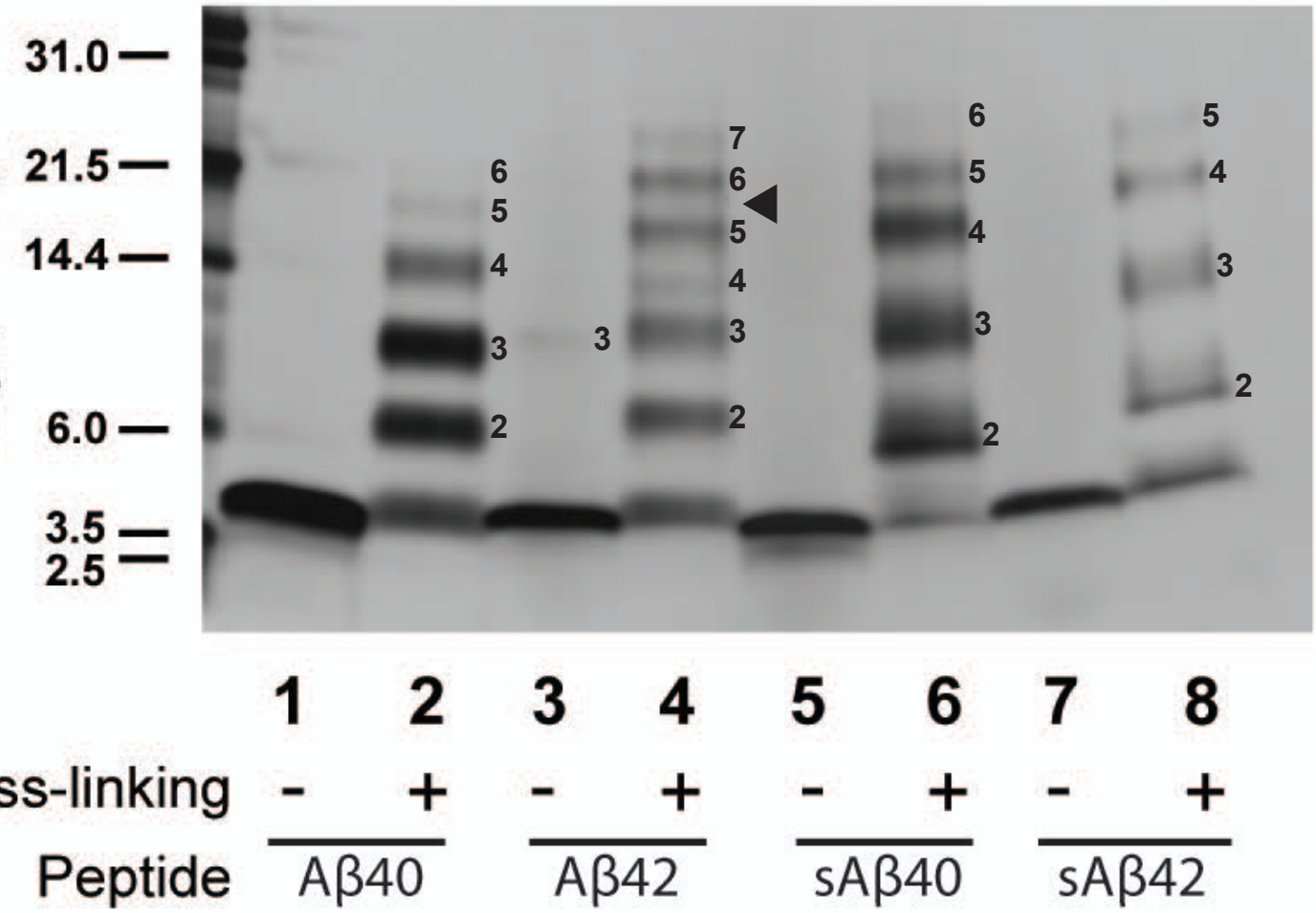

Fig. 4

Fig. 5

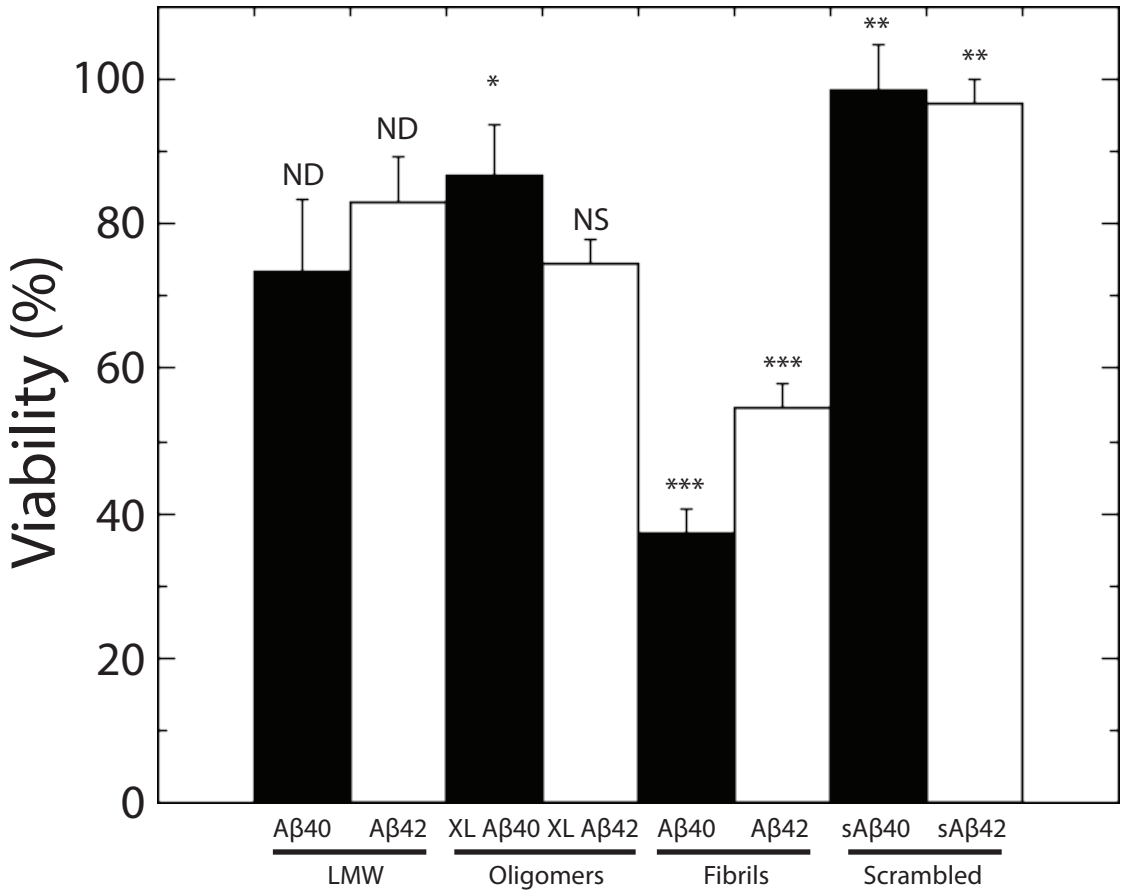
Viability (%)
100
80
60
40
20
0
ND
ND
*
NS
***
***
**
**
Aβ40
Aβ42
XL Aβ40
XL Aβ42
Aβ40
Aβ42
sAβ40
sAβ42
LMW
Oligomers
Fibrils
Scrambled

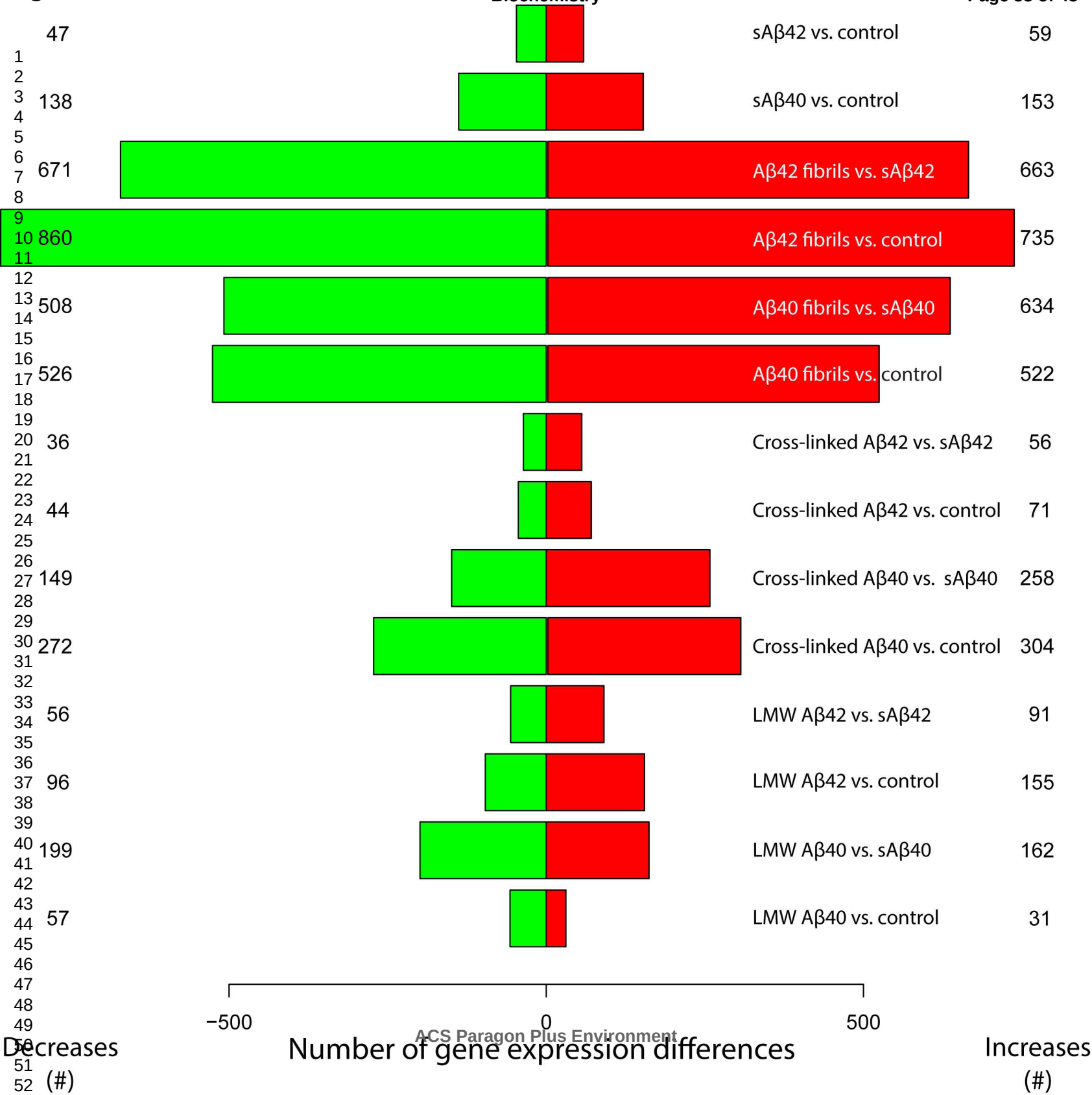

Fig. 7A

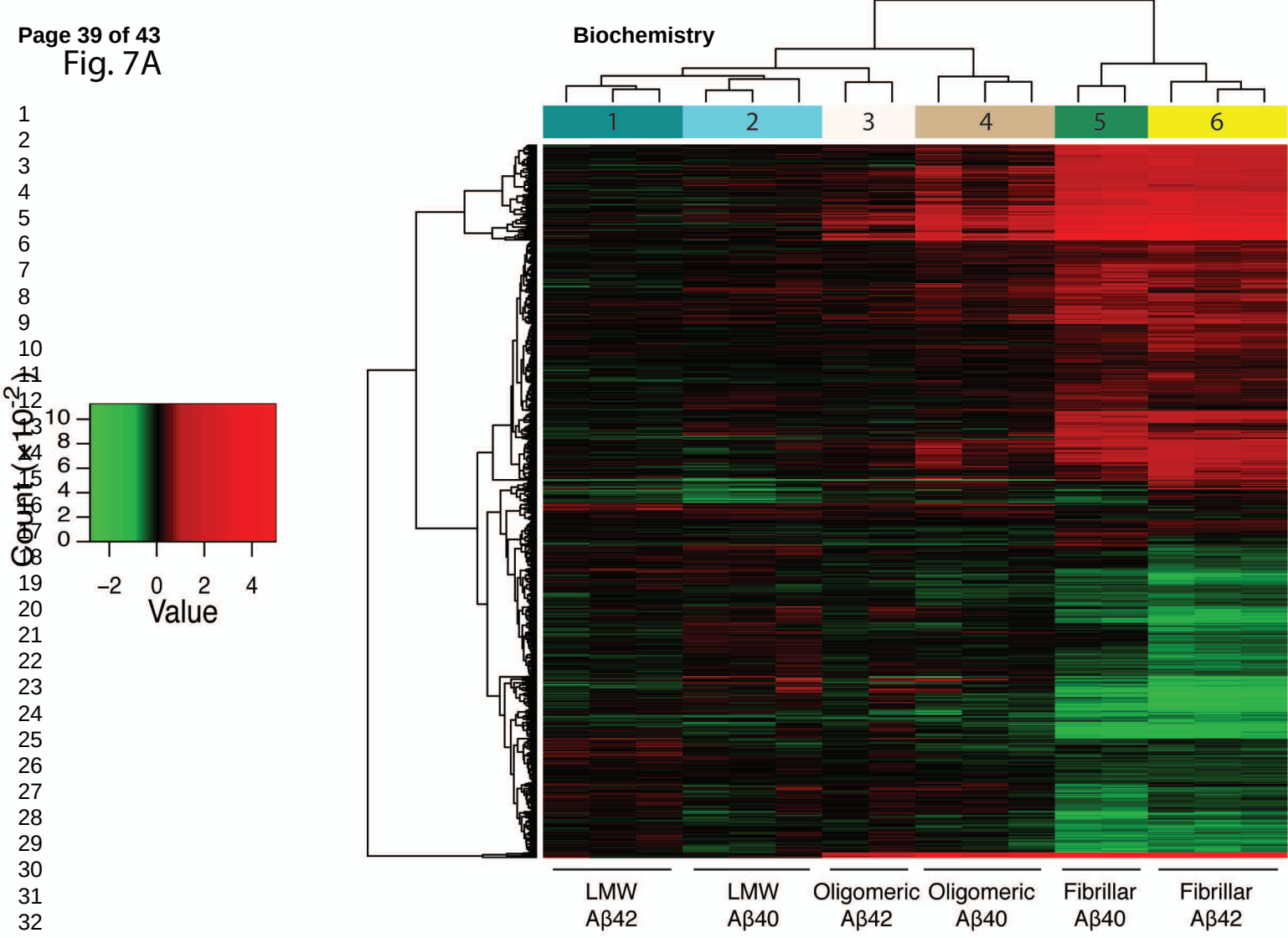
Biochemistry
1
2
3
4
5
6
Count (× 10^{-2})
10
8
6
4
2
0
−2
0
2
4
Value
LMW Aβ42
LMW Aβ40
Oligomeric Aβ42
Oligomeric Aβ40
Fibrillar Aβ40
Fibrillar Aβ42

Fig. 7B

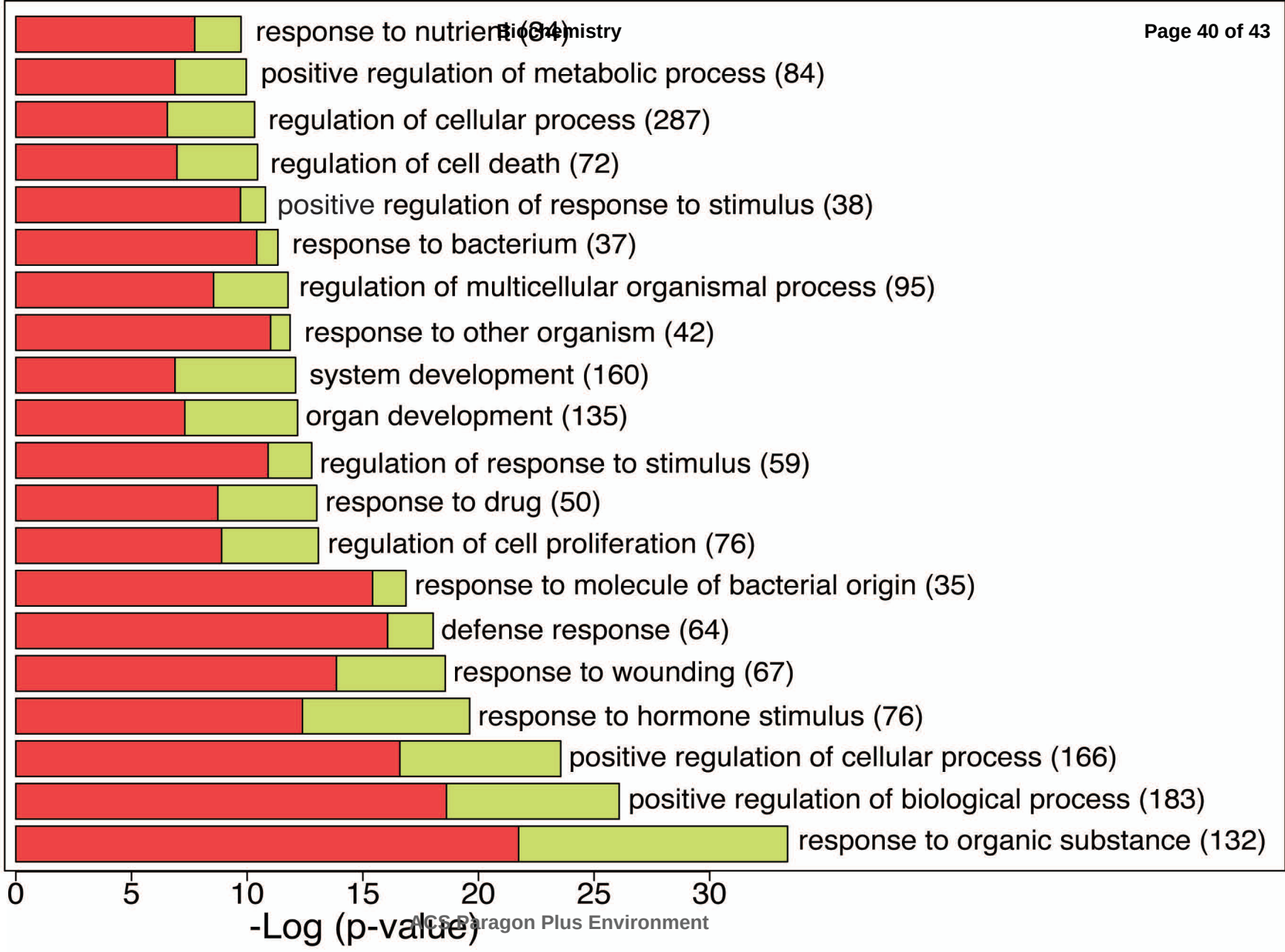

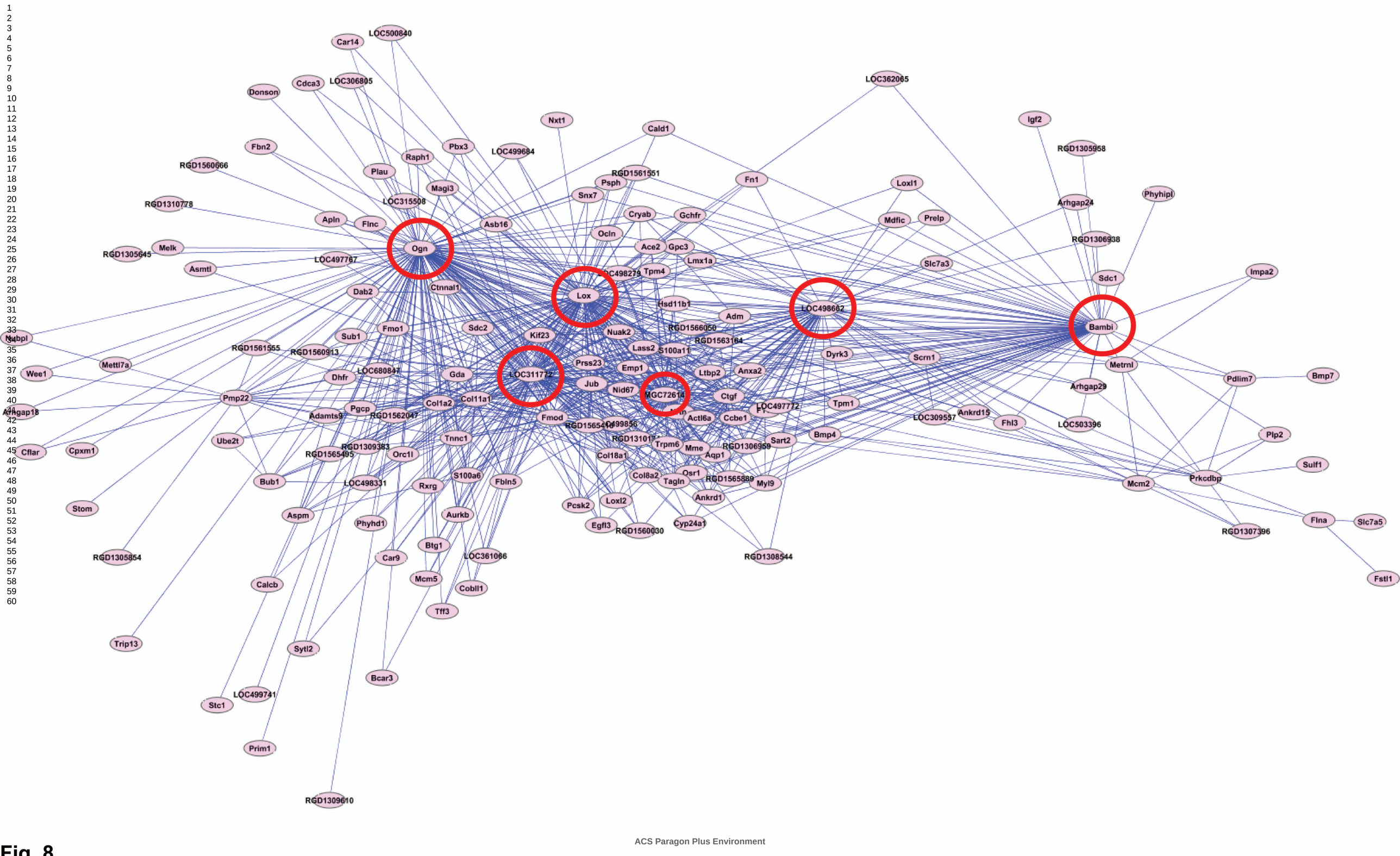
LOC500840
Car14
Cdca3
LOC306805
Donson
LOC362065
Nxt1
Cald1
Igf2
Fbn2
Pbx3
LOC499684
RGD1305958
Raph1
RGD1560666
Plau
RGD1561551
Psph
Fn1
Loxl1
Magi3
Snx7
Phyhipl
RGD1310778
LOC315508
Arhgap24
Apln
Flnc
Cryab
Gchfr
Mdfic
Prelp
Asb16
Ocln
RGD1306938
Melk
Ogn
Ace2
Gpc3
RGD1305645
LOC497767
Lmx1a
Slc7a3
Asmtl
LOC498279
Tpm4
Sdc1
Impa2
Ctnnal1
Dab2
Lox
Hsd11b1
LOC498662
Adm
Fmo1
Sdc2
RGD1566050
Bambi
Nubpl
Sub1
Kif23
Nuak2
RGD1563164
RGD1561555
RGD1560913
Lass2
S100a11
Dyrk3
Scrn1
Mettl7a
Prss23
Emp1
Ltbp2
Anxa2
Metrnl
Wee1
LOC680847
Dhfr
Gda
LOC311772
Jub
Nid67
MGC72614
Ctgf
Arhgap29
Pdlim7
Bmp7
Pmp22
Col1a2
Col11a1
Tpm1
Arhgap18
Pgcp
LOC497772
Adamts9
RGD1562047
Fmod
Actl6a
Ccbe1
LOC309557
Ankrd15
Fhl3
LOC503396
RGD1565470
LOC499856
Ube2t
Tnnc1
RGD1310177
Trpm6
Mme
Sart2
Bmp4
Plp2
Cflar
Cpxm1
RGD1309383
RGD1565495
Orc1l
Col18a1
RGD1306959
Aqp1
Sulf1
Bub1
LOC498331
S100a6
Fbln5
Col8a2
Osr1
Tagln
RGD1565889
Myl9
Mcm2
Prkcdbp
Stom
Rxrg
Pcsk2
Loxl2
Ankrd1
Aspm
Aurkb
Phyhd1
Egfl3
RGD1560030
Cyp24a1
Flna
Slc7a5
RGD1307396
RGD1305854
Btg1
Car9
LOC361066
RGD1308544
Mcm5
Cobll1
Calcb
Tff3
Fstl1
Trip13
Sytl2
Bcar3
Stc1
LOC499741
Prim1
RGD1309610

Fig. 8

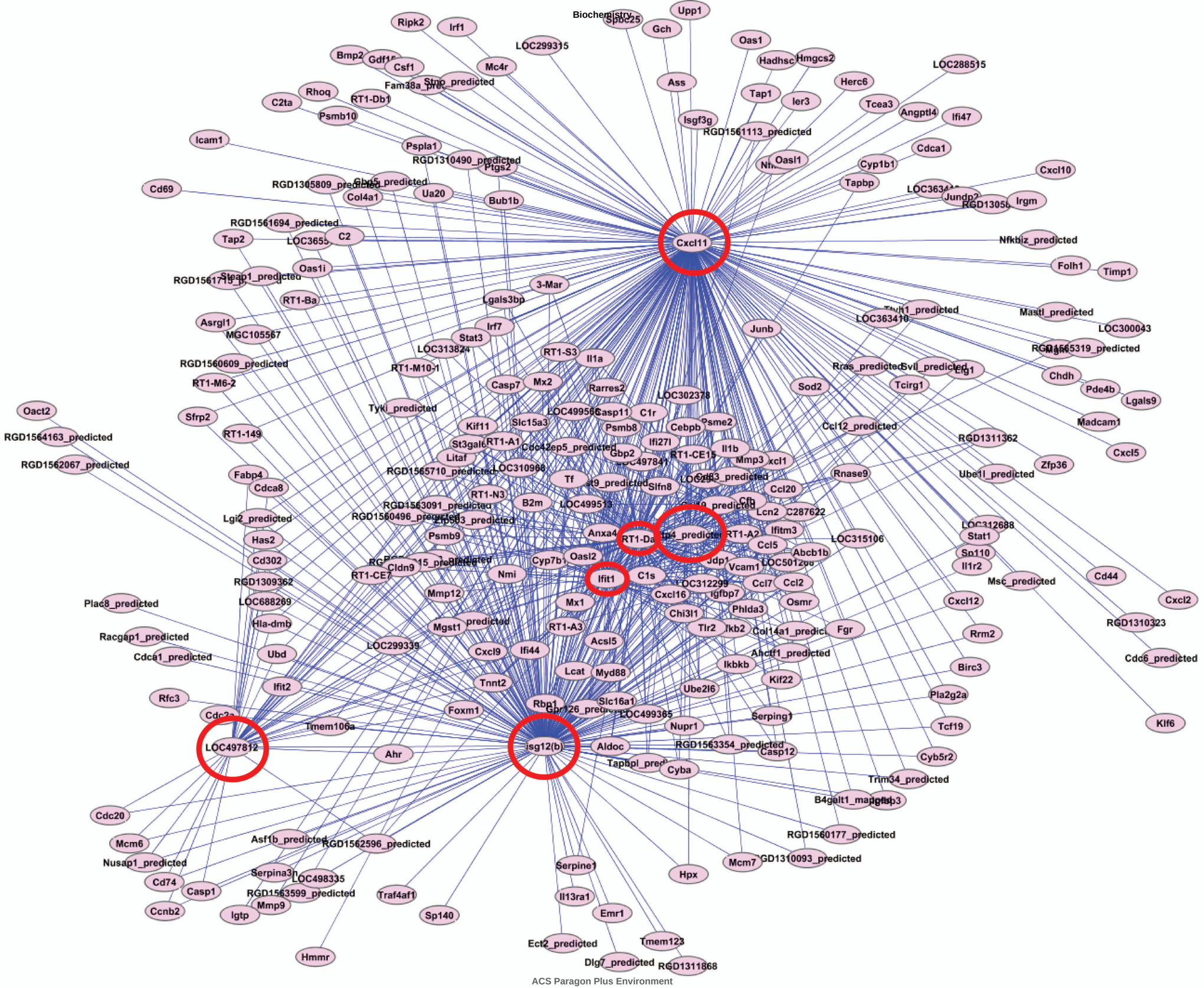

ACS Paragon Plus Environment

Fig. 9

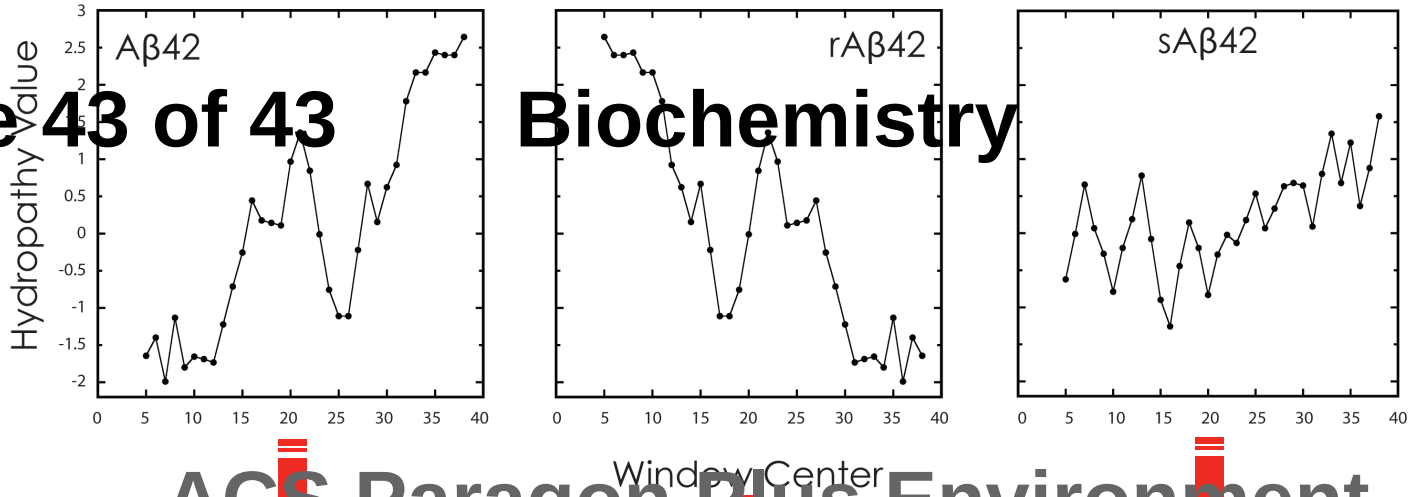

ACS Paragon Plus Environment

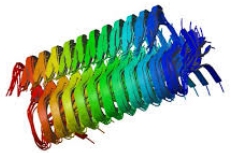

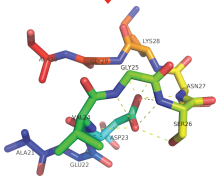

SUPPORTING INFORMATION

Design, characterization, and use of a novel amyloid β-protein control for assembly, neurotoxicity, and gene expression studies

Ghiam Yamin[a, b], Giovanni Coppola[b, c], and David B. Teplow[b*]

Table S1. Average signal intensity differences among genes after treatment with specific Aβ assemblies. (Will be available with published version.)

Table S2. Commercially available scrambled Aβ peptides.

Fig. S1. Phase-contrast microscopy image of primary hippocampal neurons after 7 days in culture. Red scale bar is 91 μm.

Fig. S2. Relationship between module eigengene (first principal component, corresponding to the weighted summation of expression across all the probes included in a given module) and treatment (Aβ assembly type). The orange and yellow modules, which are independent from one another, showed the greatest correlation with fibrillar Aβ40 and Aβ42 treatment among the total of 13 modules defined. Cont: control; S40 and S42: sAβ40 and sAβ42; T40 and T42: LMW Aβ40 and LMW Aβ42, XL40 and XL42: cross-linked Aβ40, cross-linked Aβ40 and Aβ42; F40 and F42: fibrillar Aβ40 and fibrillar Aβ42, respectively.

Table S2. Commercially available scrambled Aβ peptides

Class	Name	Sequence	References
I	Scrambled A β 40	AEGDSHVLKEGAYMEIFDVQGHVFGGKIFRVVDLGSHNVA	*1-4*
	Scrambled A β 42	AIAEGDSHVLKEGAYMEIFDVQGHVFGGKIFRVVDLGSHNVA	
II	Scrambled A β 40	KVKGLIDGAHIGDLVYEFMDSNSFREGVGAGHVHVAQVEF	*5*
	Scrambled A β 42	KVKGLIDGAHIGDLVYEFMDSNSAIFREGVGAGHVHVAQVEF	

References

[1] Giliberto, L., Borghi, R., Piccini, A., Mangerini, R., Sorbi, S., Cirmena, G., Garuti, A., Ghetti, B., Tagliavini, F., Mughal, M. R., Mattson, M. P., Zhu, X., Wang, X., Guglielmotto, M., Tamagno, E., and Tabaton, M. (2009) Mutant presenilin 1 increases the expression and activity of BACE1, *J Biol Chem 284*, 9027-9038.

[2] Maloney, M. T., Minamide, L. S., Kinley, A. W., Boyle, J. A., and Bamburg, J. R. (2005) β-secretase-cleaved amyloid precursor protein accumulates at actin inclusions induced in neurons by stress or amyloid β: a feedforward mechanism for Alzheimer's disease, *J Neurosci 25*, 11313-11321.

[3] Shaked, G. M., Kummer, M. P., Lu, D. C., Galvan, V., Bredesen, D. E., and Koo, E. H. (2006) Aβ induces cell death by direct interaction with its cognate extracellular domain on APP (APP 597-624), *FASEB J 20*, E546-E555.

[4] Ji, Y., Permanne, B., Sigurdsson, E. M., Holtzman, D. M., and Wisniewski, T. (2001) Amyloid β40/42 clearance across the blood-brain barrier following intra-ventricular injections in wild-type, apoE knock-out and human apoE3 or E4 expressing transgenic mice, *J Alzheimers Dis 3*, 23-30.

[5] Hu, J., Akama, K. T., Krafft, G. A., Chromy, B. A., and Van Eldik, L. J. (1998) Amyloid-β peptide activates cultured astrocytes: morphological alterations, cytokine induction and nitric oxide release, *Brain Res 785*, 195-206.

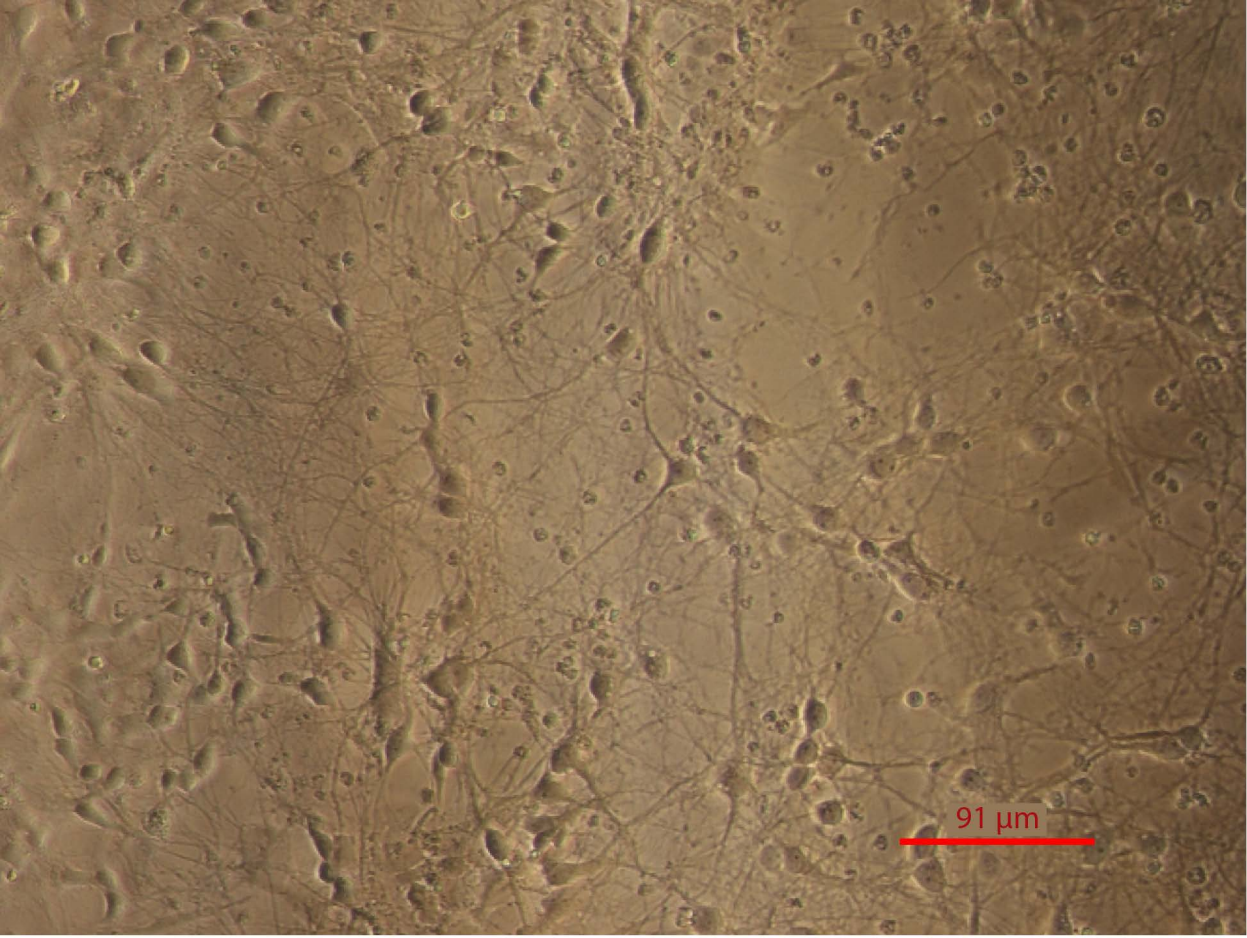

Fig. S1

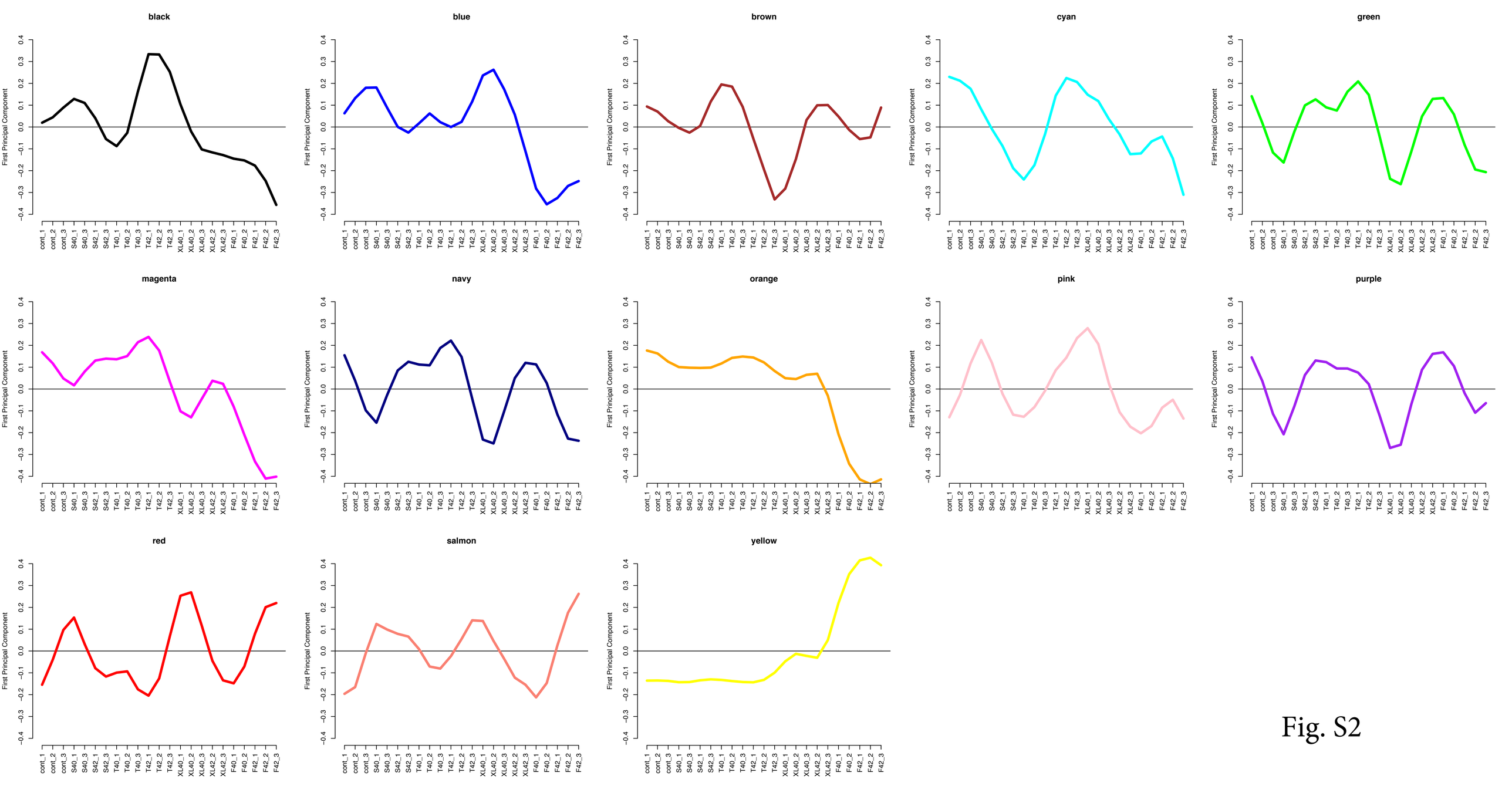
black
blue
brown
cyan
green
magenta
navy
orange
pink
purple
red
salmon
yellow
First Principal Component
cont_1
cont_2
cont_3
S40_1
S40_3
S42_1
S42_3
T40_1
T40_2
T40_3
T42_1
T42_2
T42_3
XL40_1
XL40_2
XL40_3
XL42_2
XL42_3
F40_1
F40_2
F42_1
F42_2
F42_3

Fig. S2